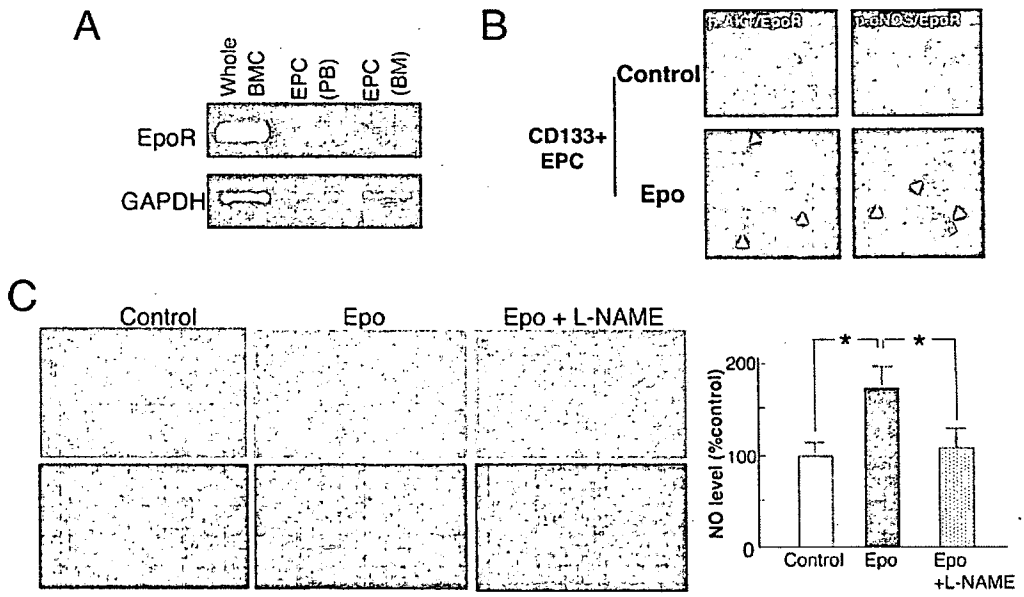

Figure 6. Epo-mediated activation of Akt/eNOS and NO production in PB-derived endothelial progenitor cells. A, The Sca1$^+$/Flk-1$^+$ EPCs were isolated from the PB and BM by FACS. Total RNAs were prepared from them and the whole BM cells and subsequently subjected to RT-PCR analysis using the primers for EpoR and GAPDH. The DNA fragments corresponding to EpoR and GAPDH were amplified in the predicted sizes. B, CD133$^+$ progenitor cells were purified to >90% purity from human PB MNCs by positive selection using anti-CD133$^+$ microbeads and a magnetic cell sorting device and then were primary cultured. After 12 hours of serum starvation (0.5% serum), they were stimulated by 1.2 IU/mL Epo for 30 minutes and immunostained for EpoR (green) with phosphorylated Akt kinase (red) or phosphorylated eNOS (red) (bar=25 μm). Double-fluorescence–positive cells appear yellow (arrowheads). C, Measurement of the intracellular NO level. The CD133$^+$ cells were loaded with DAF-FM DA (10 μmol/L), and NO was visualized as a green dot under laser microscopy. The averaged intensity in the Epo and the Epo plus L-NAME cells relative to the control group was evaluated. *P<0.005 (n=8, each).

Acknowledgments

This work was supported by a Grant from the Ministry of Education, Culture, Science and Technology of Japan.

References

1. Libby P, Schwartz D, Brogi E, Tanaka H, Clinton SK. A cascade model for restenosis. A special case of atherosclerosis progression. *Circulation.* 1992;86(suppl III):III-47–III-52.
2. Asahara T, Murohara T, Sullivan A, Silver M, van der Zee R, Li T, Witzenbichler B, Schatteman G, Isner JM. Isolation of putative progenitor endothelial cells for angiogenesis. *Science.* 1997;275:964–967.
3. Asahara T, Masuda H, Takahashi T, Kalka C, Pastore C, Silver M, Kearne M, Magner M, Isner JM. Bone marrow origin of endothelial progenitor cells responsible for postnatal vasculogenesis in physiological and pathological neovascularization. *Circ Res.* 1999;85:221–228.
4. Griese DP, Ehsan A, Melo LG, Kong D, Zhang L, Mann MJ, Pratt RE, Mulligan RC, Dzau VJ. Isolation and transplantation of autologous circulating endothelial cells into denuded vessels and prosthetic grafts: implications for cell-based vascular therapy. *Circulation.* 2003;108:2710–2715.
5. Fujiyama S, Amano K, Uehira K, Yoshida M, Nishiwaki Y, Nozawa Y, Jin D, Takai S, Miyazaki M, Egashira K, Imada T, Iwasaka T, Matsubara H. Bone marrow monocyte lineage cells adhere on injured endothelium in a monocyte chemoattractant protein-1-dependent manner and accelerate reendothelialization as endothelial progenitor cells. *Circ Res.* 2003;93:980–989.
6. Werner N, Junk S, Laufs U, Link A, Walenta K, Bohm M, Nickenig G. Intravenous transfusion of endothelial progenitor cells reduces neointima formation after vascular injury. *Circ Res.* 2003;93:e17–e24.
7. Kong D, Melo LG, Mangi AA, Zhang L, Lopez-Ilasaca M, Perrella MA, Liew CC, Pratt RE, Dzau VJ. Enhanced inhibition of neointimal hyperplasia by genetically engineered endothelial progenitor cells. *Circulation.* 2004a;109:1769–1775.
8. Gulati R, Jevremovic D, Peterson TE, Witt TA, Kleppe LS, Mueske CS, Lerman A, Vile RG, Simari RD. Autologous culture-modified mononuclear cells confer vascular protection after arterial injury. *Circulation.* 2003;108:1520–1526.
9. Anagnostou A, Liu Z, Steiner M, Chin K, Lee ES, Kessimian N, Noguchi CT. Erythropoietin receptor mRNA expression in human endothelial cells. *Proc Natl Acad Sci U S A.* 1994;91:3974–3978.
10. Anagnostou A, Lee ES, Kessimian N, Levinson R, Steiner M. Erythropoietin has a mitogenic and positive chemotactic effect on endothelial cells. *Proc Natl Acad Sci U S A.* 1990;87:5978–5982.
11. Carlini RG, Alonzo EJ, Dominguez J, Blanca I, Weisinger JR, Rothstein M, Bellorin-Font E. Effect of recombinant human erythropoietin on endothelial cell apoptosis. *Kidney Int.* 1999;55:546–553.
12. Beleslin-Cokic BB, Cokic VP, Yu X, Weksler BB, Schechter AN, Noguchi CT. Erythropoietin and hypoxia stimulate erythropoietin receptor and nitric oxide production by endothelial cells. *Blood.* 2004;103:921–926.
13. Heeschen C, Aicher A, Lehmann R, Fichtlscherer S, Vasa M, Urbich C, Mildner-Rihm C, Martin H, Zeiher AM, Dimmeler S. Erythropoietin is a potent physiologic stimulus for endothelial progenitor cell mobilization. *Blood.* 2003;102:1340–1346.
14. Ribatti D, Presta M, Vacca A, Ria R, Giuliani R, Dell'Era P, Nico B, Roncali L, Dammacco F. Human erythropoietin induces a pro-angiogenic phenotype in cultured endothelial cells and stimulates neovascularization in vivo. *Blood.* 1999;93:2627–2636.
15. Galeano M, Altavilla D, Cucinotta D, Russo GT, Calo M, Bitto A, Marini H, Marini R, Adamo EB, Seminara P, Minutoli L, Torre V, Squadrito F. Recombinant human erythropoietin stimulates angiogenesis and wound healing in the genetically diabetic mouse. *Diabetes.* 2004;53:2509–2517.
16. Kalka C, Masuda H, Takahashi T, Gordon R, Tepper O, Gravereaux E, Pieczek A, Iwaguro H, Hayashi SI, Isner JM, Asahara T. Vascular endothelial growth factor165 gene transfer augments circulating endothelial progenitor cells in human subjects. *Circ Res.* 2000;86:1198–1202.
17. Kocher AA, Schuster MD, Szabolcs MJ, Takuma S, Burkhoff D, Wang J, Homma S, Edwards NM, Itescu S. Neovascularization of ischemic myocardium by human bone-marrow-derived angioblasts prevents cardiomyocyte apoptosis, reduces remodeling and improves cardiac function. *Nat Med.* 2001;7:430–436.
18. Kong D, Melo LG, Gnecchi M, Zhang L, Mostoslavsky G, Liew CC, Pratt RE, Dzau VJ. Cytokine-induced mobilization of circulating endothelial progenitor cells enhances repair of injured arteries. *Circulation.* 2004b;110:2039–2046.

19. Sata M, Saiura A, Kunisato A, Tojo A, Okada S, Tokuhisa T, Hirai H, Makuuchi M, Hirata Y, Nagai R. Hematopoietic stem cells differentiate into vascular cells that participate in the pathogenesis of atherosclerosis. *Nat Med.* 2002;8:403–409.
20. Okabe M, Ikawa M, Kominami K, Nakanishi T, Nishimune Y. 'Green mice' as a source of ubiquitous green cells. *FEBS Lett.* 1997;407:313–319.
21. Zambrowicz BP, Imamoto A, Fiering S, Herzenberg LA, Kerr WG, Soriano P. Disruption of overlapping transcripts in the ROSA beta geo 26 gene trap strain leads to widespread expression of beta-galactosidase in mouse embryos and hematopoietic cells. *Proc Natl Acad Sci U S A.* 1997;94:3789–3794.
22. Hori T, Matsubara T, Ishibashi T, Yamazoe M, Ida T, Higuchi K, Takemoto M, Ochiai S, Tamura Y, Aizawa Y, Nishio M. Decrease of nitric oxide end-products during coronary circulation reflects elevated basal coronary artery tone in patients with vasospastic angina. *Jpn Heart J.* 2000;41:583–595.
23. Urbich C, Heeschen C, Aicher A, Sasaki K, Bruhl T, Farhadi MR, Vajkoczy P, Hofmann WK, Peters C, Pennacchio LA, Abolmaali ND, Chavakis E, Reinheckel T, Zeiher AM, Dimmeler S. Relevance of monocytic features for neovascularization capacity of circulating endothelial progenitor cells. *Circulation.* 2003;108:2511–2516.
24. Moroi M, Zhang L, Yasuda T, Virmani R, Gold HK, Fishman MC, Huang PL. Interaction of genetic deficiency of endothelial nitric oxide, gender, and pregnancy in vascular response to injury in mice. *J Clin Invest.* 1998;101:1225–1232.
25. Sata M, Maejima Y, Adachi F, Fukino K, Saiura A, Sugiura S, Aoyagi T, Imai Y, Kurihara H, Kimura K, Omata M, Makuuchi M, Hirata Y, Nagai R. A mouse model of vascular injury that induces rapid onset of medial cell apoptosis followed by reproducible neointimal hyperplasia. *J Mol Cell Cardiol.* 2000;32:2097–2104.
26. Beohar N, Flaherty JD, Davidson CJ, Maynard RC, Robbins JD, Shah AP, Choi JW, MacDonald LA, Jorgensen JP, Pinto JV, Chandra S, Klaus HM, Wang NC, Harris KR, Decker R, Bonow RO. Antirestenotic effects of a locally delivered caspase inhibitor in a balloon injury model. *Circulation.* 2004;109:108–113.
27. Hill JM, Syed MA, Arai AE, Powell TM, Paul JD, Zalos G, Read EJ, Khuu HM, Leitman SF, Horne M, Csako G, Dunbar CE, Waclawiw MA, Cannon RO 3rd. Outcomes and risks of granulocyte colony-stimulating factor in patients with coronary artery disease. *J Am Coll Cardiol.* 2005;46:1643–1648.
28. Fukumoto Y, Miyamoto T, Okamura T, Inaba S, Harada M, Niho Y. Angina pectoris occurring during granulocyte colony-stimulating factor-combined preparatory regimen for autologous peripheral blood stem cell transplantation in a patient with acute myelogenous leukaemia. *Br J Haematol.* 1997;97:666–668.
29. Kawachi Y, Watanabe A, Kurooka N, Setsu K. Acute arterial thrombosis due to platelet aggregation in a patient receiving granulocyte colony-stimulating factor. *Br J Haematol.* 1996;94:413–416.
30. Rizzo JD, Lichtin AE, Woolf SH, Seidenfeld J, Bennett CL, Regan DH, Browman GP, Gordon MS; American Society of Clinical Oncology; American Society of Hematology. Use of epoetin in patients with cancer: evidence-based clinical practice guidelines of the American Society of Clinical Oncology and the American Society of Hematology. *Blood.* 2002;100:2303–2320.
31. Vogel V, Kramer HJ, Backer A, Meyer-Lehnert H, Jelkmann W, Fandrey J. Effects of erythropoietin on endothelin-1 synthesis and the cellular calcium messenger system in vascular endothelial cells. *Am J Hypertens.* 1997;10:289–296.
32. Genc S, Koroglu TF, Genc K. Erythropoietin as a novel neuroprotectant. *Res Neurol Neurosci.* 2004;22:105–119.
33. Chong ZZ, Kang JQ, Maiese K. Erythropoietin is a novel vascular protectant through activation of Akt1 and mitochondrial modulation of cysteine proteases. *Circulation.* 2002;106:2973–2979.

Granulocyte Colony-Stimulating Factor–Mobilized Circulating c-Kit+/Flk-1+ Progenitor Cells Regenerate Endothelium and Inhibit Neointimal Hyperplasia After Vascular Injury

Michitaka Takamiya, Mitsuhiko Okigaki, Denan Jin, Shinji Takai, Yoshihisa Nozawa, Yasushi Adachi, Norifumi Urao, Kento Tateishi, Tetsuya Nomura, Kan Zen, Eishi Ashihara, Mizuo Miyazaki, Tetsuya Tatsumi, Tomosaburo Takahashi, Hiroaki Matsubara

Background—Granulocyte colony-stimulating factor (G-CSF) treatment was shown to inhibit neointimal formation of balloon-injured vessels, whereas neither the identification of progenitor cells involved in G-CSF–mediated endothelial regeneration with a bone marrow (BM) transplant experiment nor the functional properties of regenerated endothelium have been studied.

Methods and Results—Recombinant human G-CSF (100 μg/kg per day) was injected daily for 14 days starting 3 days before balloon injury in the rat carotid artery. Neointimal formation of denuded vessels on day 14 was markedly attenuated by G-CSF (39% versus the control; $P<0.05$). Endothelial cell–specific immunostaining revealed an enhancement of re-endothelialization (1.8-fold increase versus the control; $P<0.05$) and inhibition of extravasation of Evans Blue dye (47%; $P=0.02$). The regenerated endothelium exhibited acetylcholine-mediated vasodilatation in NO-dependent manner. G-CSF increased the circulating c-Kit+/Flk-1+ cells (9.1-fold; $P<0.02$), which showed endothelial properties in vitro (acetylated low-density lipoprotein uptake and lectin binding) and incorporated into the regenerated endothelium in vivo. A BM replacement experiment with green fluorescent protein (GFP)–overexpressing cells showed that BM-derived GFP+/CD31+ endothelial cells occupied 39% of the total luminal length in the G-CSF–mediated neo-endothelium (2% in the control).

Conclusion—The G-CSF–induced mobilization of BM-derived c-Kit+/Flk-1+ cells contributes to endothelial regeneration, and this cytokine therapy may be a feasible strategy for the promotion of re-endothelialization after angioplasty. **(*Arterioscler Thromb Vasc Biol.* 2006;26:751-757.)**

Key Words: restenosis ▫ endothelium ▫ carotid artery ▫ cytokines ▫ vascular biology

Endothelial cells (ECs) cover the luminal surface of blood vessels and maintain multiple vascular functions. The disruption of endothelial coverage causes a decrease in the production of vasculoprotective mediators such as NO, leading to elevated vascular tonus, enhanced inflammation, and medial smooth muscle cell proliferation. The resultant neointimal hyperplasia causes restenosis after angioplasty.[1]

Bone marrow (BM)–derived endothelial progenitor cells (EPCs) was isolated from the mononuclear cell (MNC) population in the peripheral blood (PB).[2,3] Transplantation of autologous circulating EPCs (CEPCs) to balloon-denuded arteries was reported to induce rapid re-endothelialization of the injured artery.[4,5] Moreover, transfusion of spleen-derived EPCs or EPCs overexpressing endothelial NO synthase reduced neointimal formation after vascular injury.[6,7] Delivery of cultured PB-MNCs to balloon-injured arteries accelerated re-endothelialization associated with endothelium-dependent vasoreactivity and reduced neointimal formation.[7]

Cytokines efficiently mobilize hematopoietic precursor cells from BM.[8] Takahashi et al showed that exogenous granulocyte/macrophage colony-stimulating factor (CSF) mobilize CEPCs from BM and thereby contributes to neovascularization of ischemic tissues.[9] Recently, granulocyte-CSF (G-CSF) was shown to recruit BM-derived EPCs[10] and enhance the BM cell mobilization to brain, leading to angiogenesis and eventually a reduction in the volume of cerebral infarction.[11] G-CSF was also reported to increase angiogenesis in the BM of G-CSF–treated patients.[12] Treatment with

Original received June 6, 2005; final version accepted December 15, 2005.

From the Department of Cardiovascular Medicine (M.T., M.O., N.U., K.T., T.N., K.Z., E.A., T. Tatsumi, T. Takahashi, H.M.), Kyoto Prefectural University School of Medicine, Japan; Department of Pharmacology (D.J., S.T., M.M.), Osaka Medical College, Takatsuki, Japan; Pharmacobioregulation Research Laboratory (Y.N.), Taiho Pharmaceutical Co. Ltd, Saitama, Japan; and Department of Pathology II (Y.A.), Kansai Medical University, Moriguchi, Japan.

Correspondence to Mitsuhiko Okigaki MD, Department of Cardiovascular Medicine, Kyoto Prefectural University of Medicine, Kamigyo-ku, Kyoto, 602-8566, Japan. E-mail okigakim@koto.kpu-m.ac.jp

Arterioscler Thromb Vasc Biol. is available at http://www.atvbaha.org

DOI: 10.1161/01.ATV.0000205607.98538.9a

G-CSF plus macrophage CSF accelerates neovascularization in limb ischemia.[13] G-CSF enhances endothelialization of small-caliber prosthetic implanted grafts,[14,15] and intracoronary infusion of G-CSF–mobilized PB-MNCs improved cardiac regional flow in patients with myocardial infarction.[16] Kong et al reported that mobilization of CEPCs by exogenous G-CSF facilitates re-endothelialization and inhibits neointimal development,[17] whereas the cell types of BM-derived cells contributing to G-CSF–mediated endothelial regeneration in the vascular repair model has not been defined in a BM transplant experiment, and neither the involvement of G-CSF–mediated outgrowth of resident ECs bordering the injured area nor the functional properties of the regenerated endothelium were studied in G-CSF–treated animals. To further elucidate these undetermined issues, the present study was designed, and it provided the additional novel findings that: (1) BM-derived c-Kit+/Flk-1+ progenitor cells mobilized by G-CSF directly contribute to the endothelial regeneration after EC-denuded injury and can differentiate to EC-like cells in vitro, (2) the contribution of the G-CSF–mediated outgrowth of resident ECs is negligible, and (3) the repaired artery showed NO-mediated arterial relaxation and inhibition of neointimal hyperplasia. These findings suggested that G-CSF therapy can be a feasible therapy to inhibit neointimal hyperplasia after angioplasty.

Materials and Methods

Balloon Injury Model

A 2Fr Fogarty arterial embolectomy catheter (Edwards Lifesciences) was inserted into the right common carotid artery of Lewis rats (LEW/SsN Slc; 10 to 12 weeks of age) and inflated 3 times with 300 μL of air. Human G-CSF (Lenograstim; 10, 30, or 100 μg/kg per day) or vehicle (saline) was subcutaneously injected daily for 14 days from 3 days before injury. The lesion was harvested on day 14. Green fluorescent protein (GFP) transgenic mice were generously donated by Dr Okabe (Osaka University, Japan).[18] All experimental procedures complied with the institutional guidelines for animal experiments.

Morphometric Analysis

The injured lesion was fixed with 4% paraformaldehyde, paraffin sectioned, and stained with hematoxylin and eosin or Elastica van Gieson. Three sections from each carotid artery at 300-μm intervals were analyzed with NIH image software. The absolute intimal area or relative ratio of intimal-to-medial area (I/M ratio) was evaluated. Evans blue dye (5%; Sigma) was transfused to rats 10 minutes before euthanasia to identify the remaining denuded area. Furthermore, to analyze the EC-recovered area, samples were incubated with horseradish peroxidase (HRP)–conjugated anti-FactorVIII antibody, followed by visualization with 3, 3′-diaminobenzidine (DAB). Slides were then counterstained with hematoxylin.

Functional Assay of Regenerated Endothelium

NO-mediated vasorelaxation of regenerated endothelium was evaluated as we described previously.[5]

Transfusion of G-CSF–Induced PB-MNCs

PB-MNCs were isolated by Percoll gradient centrifugation (Lymphoprep; NYCOMED) from 5-day G-CSF–treated donor rats and labeled with DiI[19] and transfused to the recipient Lewis rat after arterial injury (1×10^7 cells). After a 5-day G-CSF treatment in GFP-overexpressing mice, PB-MNCs were prepared and incubated with phycoerythrin (PE)–Cy5-conjugated anti-mouse CD45 or anti-mouse c-Kit antibodies (BD Pharmingen), as well as PE-conjugated anti-mouse Flk-1 (Becton Dickinson). GFP+/c-Kit+/Flk-1+ and GFP+/c-Kit+/Flk-1− cells were sorted and transfused to the recipient nude rats (F344/N rnu/rnu) after arterial injury. On day 14, the lesion was frozen sectioned and incubated with anti-CD31 antibody (Santa Cruz Biotechnology), followed by rhodamine-conjugated secondary antibody (DAKO).

Primary Culture of G-CSF–Induced PB-MNCs

PB-MNCs were prepared from 5-day G-CSF–treated rats and cultured on fibronectin-coated chamber slides (Becton Dickinson) for 7 days with 10% FBS-DMEM (GIBCO). Adherent cells were incubated with 2.4 μL/mL of DiI-labeled acetylated LDL (Molecular Probes) for 120 minutes, fixed with 2% paraformaldehyde, and stained with 10 ng/mL of fluorescein isothiocyanate (FITC)–conjugated Ulex europaeus agglutinin-1 (UEA-1) lectin (Sigma). The double fluorescent cells were counted in 4 randomly selected high-power fields.

Fluorescence-Activated Cell Sorter Analysis of G-CSF–Induced Mice PB-MNCs

PB-MNCs were prepared from 5-day G-CSF–treated C57BL/6 mice, incubated with PE-conjugated antibody against CD3, CD8, B220, CD11b, Ter119 or Gr-1, and FITC-conjugated anti-CD34 antibody as well as biotin-conjugated mouse antibody against Flk-1 or c-Kit, followed by activated protein C–conjugated secondary antibody (all from Pharmingen). Samples were analyzed with fluorescent-activated cell sorter (FACS) caliber using Cell Quest (Becton Dickinson).

BM Transplantation

1×10^7 BM cells from GFP-overexpressing mice were transplanted to nude rats (F344/N rnu/rnu) after 6 Gray irradiation. At week 4, arterial injury was conducted, and G-CSF (100 μg/kg per day) was injected daily for 14 days from 3 days before arterial injury. The lesions were frozen sectioned and stained with anti-CD31 antibody with rhodamine-conjugated secondary antibody (DAKO).

Immunohistochemistry

The injured lesions were paraffin sectioned at 14 days after balloon injury and immunostained with anti-rat CD45 (BD Pharmingen) and rat cross-reactive anti–interleukin-1β (IL-1β) antibodies (sc-7884; Santa Cruz Biotechnology) and HRP-conjugated secondary antibody, followed by visualization with DAB and counterstained with hematoxylin.

Statistical Analysis

Statistical analyses were performed with 1-way ANOVA followed by pairwise contrasts using Dunnett test. Data (means±SE) were considered statistically significant when P was <0.05.

Results

G-CSF Inhibits Neointimal Hyperplasia After Arterial Injury

We determined whether G-CSF treatment inhibits neointimal hyperplasia after EC-denuded balloon injury of carotid artery. Neointimal lesions developed in the vehicle-treated vessels 2 weeks after injury, whereas G-CSF treatment markedly reduced the neointimal formation in a dose-dependent manner (10 to 100 μg/kg per day; Figure 1). Morphometric analysis revealed a remarkable decrease in the neointimal area of high-dose G-CSF (100 μg/kg per day)–treated rats compared with the vehicle-treated group (39±3% decrease; n=10; $P<0.05$). The I/M ratio in G-CSF–treated rats was less than that in the vehicle-treated group (46.0±7.6% versus 84.3±7.3%; n=10; $P<0.05$; Figure 1B). Thus, it is unlikely that G-CSF directly affects the outgrowth of resident smooth

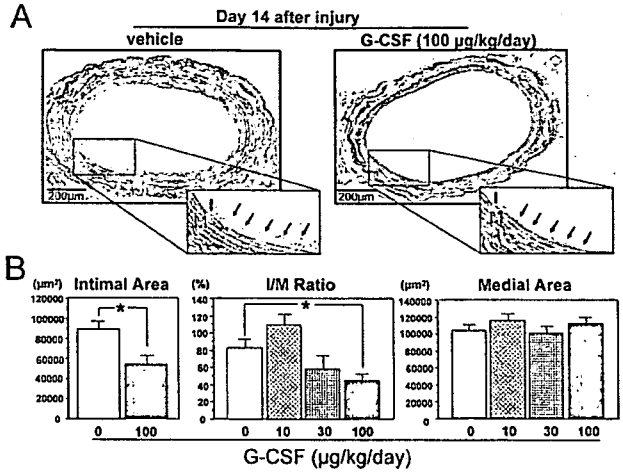

Figure 1. G-CSF inhibits neointimal hyperplasia after EC-denuded balloon injury. Endothelial denudation of rat carotid artery was induced by balloon catheter (day 0). The rats were injected with G-CSF: 0 μg/kg per day (vehicle only), 10, 30, or 100 μg/kg per day (n=10, each group). A, G-CSF (100 μg/kg per day) was subcutaneously injected daily for 14 days from 3 days before arterial injury. On day 14, the injured lesion was stained with Elastica van Gieson and subjected to morphometrical analysis. Arrows indicate apparent neointimal hyperplasia in the vehicle-injected group and marked inhibition of neointimal lesions in the G-CSF–treated group. B, Statistical analysis: intimal (I) or medial area (M) as well as the I/M ratio were evaluated 14 days after balloon injury with NIH image software. *$P<0.05$ vs vehicle-injected groups (n=10).

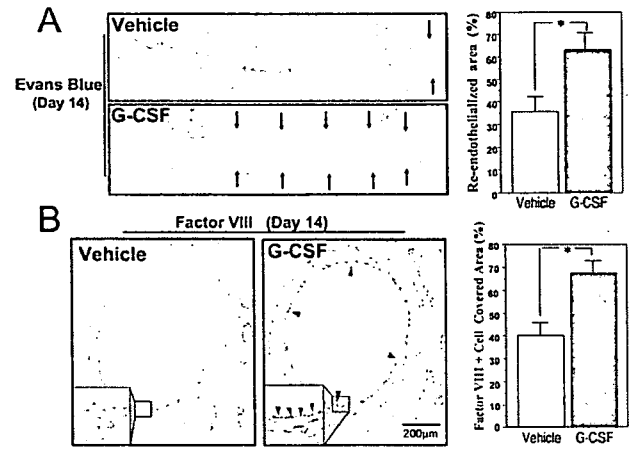

Figure 2. G-CSF facilitates re-endothelialization after EC-denuded injury. A, At 14 days after balloon injury, Evans blue dye was intravenously injected before euthanization. The re-endothelialized area, which appears white (arrows), was significantly larger in the G-CSF group than in the vehicle-treated group. *$P<0.05$ vs vehicle-injected group (n=6). B, On day 14, the injured lesion was immunostained with HRP-conjugated anti-FactorVIII antibody, followed by visualization with DAB. The FactorVIII+ cell-covered area (arrowheads) to the total length of luminal surface (%) in the G-CSF–treated group was significantly greater than in the vehicle-injected group. *$P<0.05$ vs vehicle-treated group (n=6).

muscle cells in the injured artery in vivo, although G-CSF was reported to stimulate the growth of the cultured vascular smooth muscle cells.[20]

We also studied whether G-CSF aggravated inflammatory cell infiltration and cytokine expression in the injured arteries by examining the infiltration of inflammatory cells (CD45+ cells) and the expression of inflammatory cytokine (IL-1β) in the injured arteries. Figure I (available online at http://atvb.ahajournals.org) shows that the infiltration of CD45+ cells and the expression of IL-1β are markedly inhibited in the day-14 neoendothelium of G-CSF–treated rats compared with those in the saline-treated controls, consistent with the previous observation that G-CSF pellet–induced angiogenic activity on the cornea occurred without any sign of inflammatory reactions.[21]

G-CSF treatment dose dependently (10, 30, and 100 μg/kg per day) elevated the number of white blood cells 14 days after treatment (14 500±2000, 19 660±430, 33 520±2171 cells; n=15 each), which were significantly higher compared with the vehicle-injected control (3640±153; n=15; $P<0.01$). Any dose of G-CSF (10, 30, or 100 μg/kg per day) did not affect the survival rate and body weight of the administrated rats and did not cause any macroanatomic change. Because 100 μg/kg per day of human G-CSF used here is considered to be similar to the human clinical dose based on the species difference between human and rodents,[22] and therefore this dose was used in the following experiment.

G-CSF Promotes Re-Endothelialization

To evaluate re-endothelialization, Evans Blue dye was administered premortem to stain-remaining nonendothelialized areas. Re-endothelialized areas appear white (Figure 2A) and were significantly larger in G-CSF–treated rats than in the vehicle-injected group (63.0±6.8% versus 35.7±6.6%; n=10; $P<0.01$). Immunostaining revealed that the ratio of FactorVIII+ endothelial layer relative to the total luminal surface was significantly greater in G-CSF–treated rats than in the control (67.4±7.9% versus 40.2±6.9%; n=10; $P<0.01$; Figure 2B), indicating that G-CSF promoted re-endothelialization, leading to the inhibition of neointimal hyperplasia.

Functional Analysis of Regenerated Endothelium

NO production in the regenerated endothelium was measured by acetylcholine (Ach)-mediated relaxation of carotid artery preconstricted by norepinephrine. Ach caused a relaxation response in the normal carotid artery (30.9±1.8%, n=6) versus papaverine-induced maximal relaxation in an NO-dependent manner (as shown by N^G-nitro-L-arginine methyl ester [L-NAME] inhibition), whereas in the EC-injured artery, this response was markedly abolished (2.8±0.9%, n=6). In contrast, in the G-CSF–treated injured artery, relaxation was restored to a level comparable to that of normal carotid artery (43.8±4.5%; n=6), whereas L-NAME pretreatment completely inhibited such an Ach-mediated response (Figure 3), suggesting that the regenerated endothelium exerts an NO-mediated vasorelaxation response.

Endothelial Regeneration by G-CSF–Mobilized CEPCs

Because G-CSF was reported to increase CEPCs,[10,17] we next examined whether the G-CSF–mobilized CEPCs actually contributed to endothelial regeneration after EC-denuded injury. PB-MNCs (1×10^7 cells) were prepared from 5-day

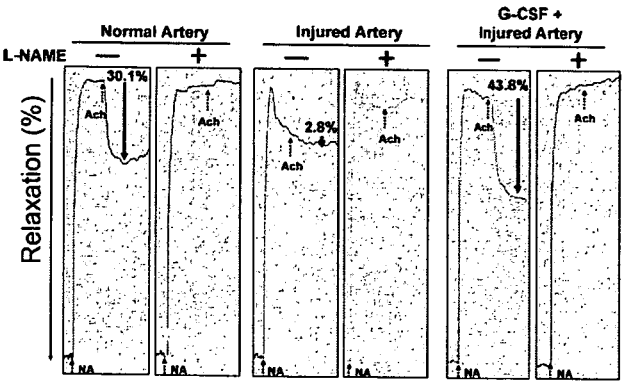

Figure 3. Ach-mediated relaxation of the carotid artery. Ach (10 μmol/L)-induced relaxation was examined using the carotid artery preconstricted with norepinephrine (30 nmol/L). The relaxation response was evaluated as a value relative to the papaverine-induced maximal relaxation (%) with or without L-NAME. Broken arrows show the time points to indicate drug administration. Solid arrows indicate Ach-induced vasorelaxation. Experiments were repeated 3 times with reproducible results. Representative data are shown.

G-CSF–treated or vehicle-injected donor rats, DiI-labeled, and transfused into the recipient rats after vascular injury. In the day-14 samples, DiI+ cells were incorporated into the neo-endothelium and double immunofluorescence with anti-CD31 antibody disclosed that DiI+ PB-MNCs derived from G-CSF–treated donor rats contributed to neoendothelium formation greater than the vehicle-injected rats (DiI+/CD31+ area 54.3±6.1% versus 6.3±1.2% to total luminal surface length; n=5; $P<0.01$; Figure 4A).

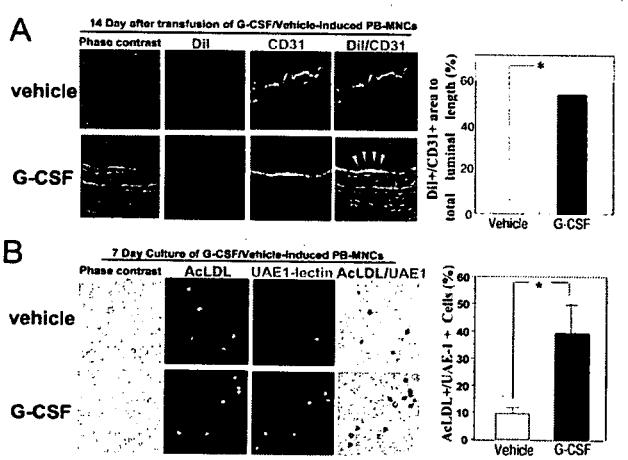

Figure 4. G-CSF increased the number of CEPCs. A, PB-MNCs were isolated from 5-day G-CSF–treated donor rats and labeled with DiI and transfused to the recipient rat after arterial injury (1×10^7 cells). On day 14, the injured lesion was removed, frozen-sectioned, and immunostained with FITC-conjugated anti-CD31 antibody. Localization of CD31+/DiI+ cells is indicated as yellow fluorescence in the merged image (arrowheads). Statistics: DiI+/CD31+ double fluorescent area in G-CSF–treated rat is greater than the vehicle-injected rat. *$P<0.05$ vs vehicle-treated group (n=6). B, PB-MNCs were cultured on fibronectin-coated plates for 7 days. EPC was identified with its binding ability to FITC–UAE-1-lectin and incorporation of DiI-AcLDL. Localization of UAE-1+/AcLDL+ cells is indicated by arrowheads in the merged image. Statistics: Percentage of double fluorescent cells relative to total adherent cells is presented (n=5; *$P<0.05$).

PB-MNCs from G-CSF–treated or vehicle-injected rats were primarily cultured for 7 days. EPC-like cells were identified by their binding ability to FITC–UEA1-lectin and uptake of DiI–AcLDL. The ratio of UAE-1+/AcLDL+ cells to total adherent cells from G-CSF–treated rats was 4-fold higher than that from vehicle-injected rats (39.2±9.8% versus 9.5±5.0% to total cultured cells; n=6; $P<0.05$; Figure 4B).

Endothelial Regeneration by G-CSF–Mobilized c-Kit+/Flk-1+ Cells

We studied the cell type responsible for endothelial regeneration induced by G-CSF. Because the anti-rat Flk-1 antibody for FACS sorting was not available, we analyzed the PB from "mice." Hematopoietic lineage negative (Lin-)/c-Kit+ cells were sorted from the mice PB and further analyzed for the expression of endothelial lineage markers Flk-1 and CD34. G-CSF treatment markedly elevated the ratio of Lin-/c-Kit+ cells to total PB-MNCs (8.1±0.5-fold; n=5; $P<0.01$), whereas the CD34+/Flk-1+ population included in the Lin-/c-Kit+ cells was increased 9.8±0.8-fold (n=5; $P<0.01$; Figure 5A).

To further elucidate the contribution of circulating c-Kit+/Flk-1+ cells to endothelial regeneration, 5×10^4 c-Kit+/Flk-1+/GFP+ or 1×10^6 c-Kit+/Flk-1-/GFP+ cells were isolated from enhanced GFP (EGFP) transgenic mice and injected into the nude rats after balloon injury. GFP mRNA transcription in the transgenic mice is driven by the chicken β-actin promoter and cytomegalovirus enhancer, indicating that the transcript expression in the hematopoietic and EC lineages is strong enough to trace them in the recipient mouse organ. In fact, GFP-positive ECs can be detected with a strong signal in the neo-endothelium. Figure 5B shows that GFP+ cells in the day-14 samples were detected on the regenerated endothelium of c-Kit+/Flk-1+ cell–transfused nude rats, and that these GFP+ cells were positive for the EC marker CD31 (Figure 5B, top, arrowheads), whereas the GFP+ cells were barely detectable in c-Kit+/Flk-1− cell–transfused nude rats (Figure 5B, bottom), suggesting that c-Kit+/Flk-1+ cells contain the cell population that can differentiate into CD31+ EC-like cells in the EC-denuded lesion.

Analysis by BM Replacement Model

To examine whether G-CSF–mobilized EPCs were originated from the BM, BM cells from EGFP transgenic mice were transplanted into the nude rats of which marrow cells had been ablated with whole body irradiation. Six weeks after transplantation, 86±2% of PB-MNCs were replaced (FACS; data not shown). The nude rats that received arterial injury and mobilization of BM-derived GFP+ cells to the neo-endothelium was examined on day 14. GFP+ cells were detected in the endothelial layer, and the immunostaining disclosed that CD31+/GFP+ EC-like cells were detected only in the G-CSF–treated group but not in the vehicle-injected group (39.2±5.8% versus 2.2±1.5% to total luminal surface length; n=5 each; $P<0.005$; Figure 6), indicating that 37.0% of the total luminal area (39.2% G-CSF group)−(2.2% saline group) was derived from G-CSF–mobilized BM cells (GFP+/CD31+ area). Considering that G-CSF–promoted neo-endothelium was 37.2% of the total luminal area (67.4%

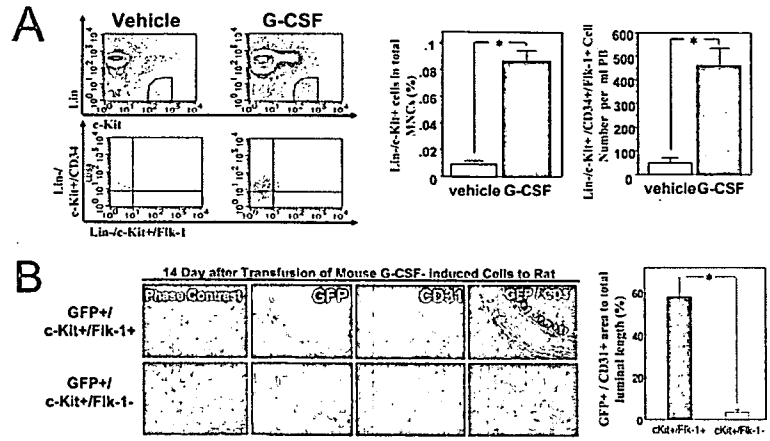

Figure 5. G-CSF–induced circulating c-Kit+/Flk-1+ cells differentiate to EC-like cells in the neo-endothelium. A, Five days after the injection of G-CSF, PB-MNCs were isolated, incubated with monoclonal antibodies (CD3-FITC, B220-FITC, CD11b-FITC, Gr1-FITC, NK1.1-FITC, Ter119-FITC, VEGFR-2-PE, and c-Kit-PE-Cy5) or with CD34-biotin, followed by activated protein C–avidine conjugated secondary antibody, and subjected to FACS analysis. The Lin-/c-Kit+ cell population was once gated (top left column) and subsequently analyzed for the expression of CD34 and Flk-1 (bottom left column). Statistical analysis: Percentage of Lin-/c-Kit+ cells to total MNCs or the absolute number of Lin-/c-Kit+/CD34+/Flk-1+ (right 2 panels) is significantly higher in G-CSF–treated group (n=5; *P<0.01 vs vehicle-injected group). B, Five days after the injection of G-CSF to GFP-overexpressing mice, PB-MNCs were collected, and 5×10^4 GFP+/c-Kit+/Flk-1+ or 1×10^6 GFP+/c-Kit+/Flk-1− cells were sorted and transfused to the nude rats after balloon injury. The lesion was removed on day 14, frozen sectioned, and subjected to immunostaining with rhodamine-conjugated antibody against CD31. CD31+/GFP+ cells appeared yellow in the merged image (arrowheads). *P<0.01 vs vehicle-treated group (n=5).

G-CSF group)−(40.2% saline group), these findings suggest that BM-derived cells are mainly involved in G-CSF–promoted neoendothelial formation, and the contribution of the G-CSF–mediated outgrowth of resident ECs is negligible.

Discussion

Because the natural regenerative process after EC-denuded injury is slow, it cannot prevent the onset of the neointimal lesions.[1] A novel approach that promotes re-endothelialization is required to accelerate this process. Several reports have shown that EPCs can be harvested from PB, and the intravenous injection of EPCs into EC-denuded vessels accelerates the recovery of endothelial integrity, resulting in the inhibition of neointimal hyperplasia and the restoration of vasodilatation activity.[4–7] The EPCs were shown to enhance the endothelialization of small-caliber prosthetic grafts.[14,15] G-CSF treatment increases the circulating CD34+ cells expressing endothelial markers,[10] and administration of G-CSF to patients with coronary artery disease increased the circulating MNCs with EPC properties.[23] Furthermore, G-CSF inhibited the neointimal formation in balloon-injured vessels,[17] whereas it remains undetermined what cell types of marrow-derived cells are directly involved in G-CSF–mediated endothelial regeneration. Furthermore, neither the functional properties of the regenerated endothelium were studied nor analysis using BM transplant experiments undertaken in G-CSF–treated animals. Our present study performed BM replacement experiments and clearly showed that G-CSF treatment increases the number of BM-derived c-Kit+/Flk-1+ EPCs that actually contribute to re-endothelialization of the balloon-injured arteries, leading to marked inhibition of neointimal formation. Furthermore, we found that the regenerated endothelium exerts Ach-mediated vasodilatory action in an NO-dependent manner. Interestingly, the injured arteries of G-CSF–treated rats have a better vasodilatory capacity compared with normal arteries. The data were analyzed in the 6 different animals with the reproducibility. Although we cannot sufficiently explain the molecular mechanism responsible for the better vasodilatory capacity, the neo-endothelium regenerated by G-CSF–mobilized BM cells or G-CSF–mediated direct action to the endothelial regeneration process might have the enhanced NO-mediated vasodilatory effect. Further studies will be required to clarify the underlying

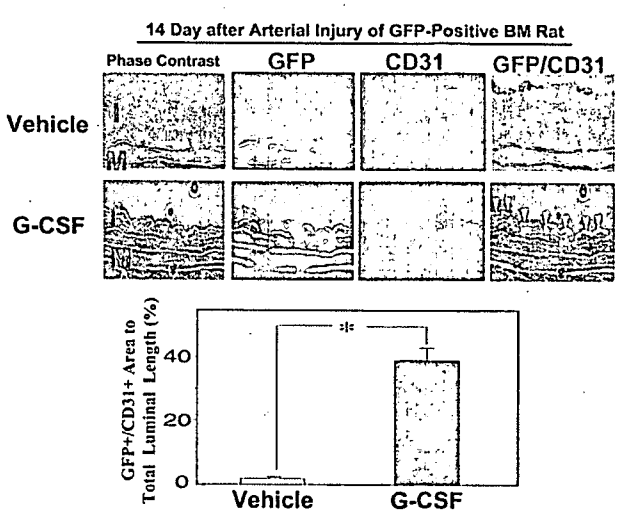

Figure 6. G-CSF–induced regenerated endothelium was originated from BM. Donor BM from EGFP-overexpressing mice was transfused to the BM-ablated nude rats. Recipient rats were balloon injured, and G-CSF or vehicle was injected daily for 14 days from 3 days before arterial injury. On day 14, the lesions were removed and immunostained with rhodamine-conjugated anti-CD31 antibody. CD31+/GFP+ cells appeared yellow in the merged image (arrowheads). Double fluorescent cells were detected on the neoendothelium in the G-CSF–treated nude rats (bottom panels), whereas they were barely detectable in the vehicle-treated nude rats (top panels). *P<0.005 vs vehicle-treated group (n=5).

mechanism. Together, this evidence leads us to consider a more aggressive clinical use of G-CSF to mobilize CEPCs and promote vascular repair.

It appears that the safety and feasibility of G-CSF treatment focusing on the induction of vascular occlusion in atherosclerotic lesions has not yet been established.[24] In angina patients, the administration of G-CSF was associated with the onset of acute myocardial infarction (AMI).[25] A high rate of restenosis after intracoronary infusion of G-CSF–mobilized PB-MNCs was reported in AMI patients.[16] There are articles reporting the induction of AMI and cerebral infarction in G-CSF–treated BM transplantation patients.[26,27] Differentiation of G-CSF–mobilized progenitor cells into smooth muscle cells within the stented segment as well as the induction of angiogenesis within the atherosclerotic lesion and the aggregation of mobilized inflammatory cells within the plaque may be a plausible explanation.[24] Furthermore, G-SCF–mobilized neutrophils may cause EC damage by superoxide production.[28–30] We have previously shown that polymorphonuclear cells inhibited the ischemia-induced recovery of blood perfusion in the hindlimb ischemia model.[31] Furthermore, G-CSF induces the expression of adhesion molecules on ECs, leading to leukocyte adhesion and its activation[32] or to a hypercoagulability state.[33] Thus, because G-CSF induces non-EPC populations, including neutrophil or smooth muscle progenitor cells, the enrichment of the EPC population and their application are required to inhibit such harmful effects. Indeed, the injection of G-CSF–induced circulating CD34+EPCs into ischemic limb muscle resulted in satisfactory clinical improvement.[34] Transplantation of an enriched CD34+MNC population re-established endothelial integrity in injured vessels, thereby inhibiting neointimal hyperplasia.[4] We here described that a small number (5×10^4) of enriched population c-Kit+/Flk-1+ or CD45-/Flk-1+ EPCs regenerated endothelium much more efficiently than did a large number (1×10^6) of c-Kit+/Flk-1− or CD45-/Flk-1− cells. Consistent with our observation, in the hindlimb ischemia model of mice, merely 1×10^3 CD34+/Flk-1+ cells improved limb salvage and hemodynamic recovery better than 1×10^4 CD34+/Flk-1− cells.[35] Thus, the application of an enriched EPC population may be feasible to improve the safety and efficiency of G-CSF therapy.

Increasing evidence suggests that BM-derived EPCs home to the ischemic region for the formation of new blood vessels.[2] EPCs were reportedly derived from more differentiated CD34+ or immature CD133+ hematopoietic stem cells, as well as from mature PB-MNCs or CD14+ monocytes.[5,36] They express endothelial markers, including Flk-1, FactorVIII, and endothelial NO synthase.[2,36] Intravenous infusion of BM-derived EPCs enhanced neovascularization in vivo.[37] Application of either BM-derived or PB-derived EPCs into the infarct artery beneficially affects postinfarction remodeling.[38,39] Consistent with these previous reports, we presented the data indicating that the c-Kit+/Flk-1+ cells were actually mobilized by G-CSF administration (Figure 5A), and the infusion experiment of the sorted c-Kit+/Flk-1+ EGFP cells (mobilized by G-CSF) revealed their direct involvement in the G-CSF–promoted endothelial regeneration process in the vascular repair. Thus, the stem cells expressing the Flk-1 marker are mobilized in response to G-CSF and then exert the property as an endothelial progenitor, suggesting that c-Kit+/Flk-1+ cells are the cell type responsible for G-CSF–mediated endothelial regeneration.

In conclusion, we characterized the cell type responsible for G-CSF–mediated endothelial regeneration leading to an inhibition of neointimal hyperplasia and showed that the vascular repair was mainly attributable to the G-CSF–mobilized BM-derived cells rather than G-CSF–mediated outgrowth of resident ECs, and that the repaired artery responded well to NO-mediated vasodilatory stimulus. These findings suggest that the treatment with G-CSF might be a feasible and suitable supplement therapy for the prevention of restenosis after the revascularization procedures. Although the very recent clinical study has reported that administration of G-CSF to patients with AMI improves cardiac function without any adverse events during 6-month observation,[40] G-CSF–mediated proatherogenic effects, such as the induction of angiogenesis within the atherosclerotic lesion and the aggregation of mobilized inflammatory cells within the atheromatous plaque, are the limitation of the present study and remain to be determined. Further basic and clinical studies focusing on these issues will be required.

Acknowledgments

This work was supported in part by a grant from the Ministry of Education, Culture, Science and Technology of Japan. We appreciate Dr Takeshi Todo for his great help in BM replacement experiment.

References

1. Libby P, Schwartz D, Brogi E, Tanaka H, Clinton SK. A cascade model for restenosis. A special case of atherosclerosis progression. *Circulation.* 1992;86:III47–III52.
2. Asahara T, Murohara T, Sullivan A, Silver M, van der Zee R, Li T, Witzenbichler B, Schatteman G, Isner JM. Isolation of putative progenitor endothelial cells for angiogenesis. *Science.* 1997;275:964–967.
3. Asahara T, Masuda H, Takahashi T, Kalka C, Pastore C, Silver M, Kearne M, Magner M, Isner JM. Bone marrow origin of endothelial progenitor cells responsible for postnatal vasculogenesis in physiological and pathological neovascularization. *Circ Res.* 1999;85:221–228.
4. Griese DP, Ehsan A, Melo LG, Kong D, Zhang L, Mann MJ, Pratt RE, Mulligan RC, Dzau VJ. Isolation and transplantation of autologous circulating endothelial cells into denuded vessels and prosthetic grafts: implications for cell-based vascular therapy. *Circulation.* 2003;108:2710–2715.
5. Fujiyama S, Amano K, Uchira K, Yoshida M, Nishiwaki Y, Nozawa Y, Jin D, Takai S, Miyazaki M, Egashira K, Imada T, Iwasaka T, Matsubara H. Bone marrow monocyte lineage cells adhere on injured endothelium in a monocyte chemoattractant protein-1-dependent manner and accelerate reendothelialization as endothelial progenitor cells. *Circ Res.* 2003;93:980–989.
6. Werner N, Junk S, Laufs U, Link A, Walenta K, Bohm M, Nickenig G. Intravenous transfusion of endothelial progenitor cells reduces neointima formation after vascular injury. *Circ Res.* 2003;93:e17–24.
7. Gulati R, Jevremovic D, Peterson TE, Witt TA, Kleppe LS, Mueske CS, Lerman A, Vile RG, Simari RD. Autologous culture-modified mononuclear cells confer vascular protection after arterial injury. *Circulation.* 2003;108:1520–1526.
8. Lapidot T, Petit I. Current understanding of stem cell mobilization: the roles of chemokines, proteolytic enzymes, adhesion molecules, cytokines, and stromal cells. *Exp Hematol.* 2002;30:973–981
9. Takahashi T, Kalka C, Masuda H, Chen D, Silver M, Kearney M, Magner M, Isner JM, Asahara T. Ischemia- and cytokine-induced mobilization of bone marrow-derived endothelial progenitor cells for neovascularization. *Nat Med.* 1999;5:434–438.
10. Kocher AA, Schuster MD, Szabolcs MJ, Takuma S, Burkhoff D, Wang J, Homma S, Edwards NM, Itescu S. Neovascularization of ischemic

myocardium by human bone-marrow-derived angioblasts prevents cardiomyocyte apoptosis, reduces remodeling and improves cardiac function. *Nat Med.* 2001;7:430–436.
11. Shyu WC, Lin SZ, Yang HI, Tzeng YS, Pang CY, Yen PS, Li H. Functional recovery of stroke rats induced by granulocyte colony-stimulating factor-stimulated stem cells. *Circulation.* 2004;110: 1847–1854.
12. Cotter M, Gulmann C, Jeffers M, Smith OP. Increased bone marrow angiogenesis in children with severe chronic neutropenia treated with granulocyte colony-stimulating factor. *J Pediatr Hematol Oncol.* 2004; 26:504–506.
13. Minamino K, Adachi Y, Okigaki M, Ito H, Togawa Y, Fujita K, Tomita M, Suzuki Y, Zhang Y, Iwasaki M, Nakano K, Koike Y, Matsubara H, Iwasaka T, Matsumura M, Ikehara S. Macrophage colony-stimulating factor (M-CSF), as well as granulocyte colony-stimulating factor (G-CSF), accelerates neovascularization. *Stem Cells.* 2005;23:347–354.
14. Bhattacharya V, Shi Q, Ishida A, Sauvage LR, Hammond WP, Wu MH. Administration of granulocyte colony-stimulating factor enhances endothelialization and microvessel formation in small caliber synthetic vascular grafts. *J Vasc Surg.* 2000;32:116–123.
15. Shi Q, Bhattacharya V, Hong-De Wu M, Sauvage LR. Utilizing granulocyte colony-stimulating factor to enhance vascular graft endothelialization from circulating blood cells. *Ann Vasc Surg.* 2002;16:314–320.
16. Kang HJ, Kim HS, Zhang SY, Park KW, Cho HJ, Koo BK, Kim YJ, Soo Lee D, Sohn DW, Han KS, Oh BH, Lee MM, Park YB. Effects of intracoronary infusion of peripheral blood stem-cells mobilised with granulocyte-colony stimulating factor on left ventricular systolic function and restenosis after coronary stenting in myocardial infarction: the MAGIC cell randomised clinical trial. *Lancet.* 2004;363:751–756.
17. Kong D, Melo LG, Mangi AA, Zhang L, Lopez-Ilasaca M, Perrella MA, Liew CC, Pratt RE, Dzau VJ. Cytokine-induced mobilization of circulating endothelial progenitor cells enhances repair of injured arteries. *Circulation.* 2004;110:2039–2046.
18. Okabe M, Ikawa M, Kominami K, Nakanishi T, Nishimune Y. 'Green mice' as a source of ubiquitous green cells. *FEBS Lett.* 1997;407: 313–319.
19. Minatoguchi S, Takemura G, Chen XH, Wang N, Uno Y, Koda M, Arai M, Misao Y, Lu C, Suzuki K, Goto K, Komada A, Takahashi T, Kosai K, Fujiwara T, Fujiwara H. Acceleration of the healing process and myocardial regeneration may be important as a mechanism of improvement of cardiac function and remodeling by postinfarction granulocyte colony–stimulating factor treatment. *Circulation.* 2004;109:2572–2580.
20. Chen X, Kelemen SE, Autieri MV. Expression of granulocyte colony-stimulating factor is induced in injured rat carotid arteries and mediates vascular smooth muscle cell migration. *Am J Physiol Cell Physiol.* 2005; 288:C81–C88.
21. Bussolino F, Ziche M, Wang JM, Alessi D, Morbidelli L, Cremona O, Bosia A, Marchisio PC, Mantovani A. In vitro and in vivo activation of endothelial cells by colony-stimulating factors. *J Clin Invest.* 1991;87: 986–995.
22. Sudo Y, Shimazaki C, Ashihara E, Kikuta T, Hirai H, Sumikuma T, Yamagata N, Goto H, Inaba T, Fujita N, Nakagawa M. Synergistic effect of FLT-3 ligand on the granulocyte colony-stimulating factor-induced mobilization of hematopoietic stem cells and progenitor cells into blood in mice. *Blood.* 1997;89:3186–3191.
23. Powell TM, Paul JD, Hill JM, Thompson M, Benjamin M, Rodrigo M, McCoy JP, Read EJ, Khuu HM, Leitman SF, Finkel T, Cannon RO III. Granulocyte colony-stimulating factor mobilizes functional endothelial progenitor cells in patients with coronary artery disease. *Arterioscler Thromb Vasc Biol.* 2005;25: 296–301.
24. Matsuabara H. Risk to the coronary arteries of intracoronary stem cell infusion and G-CSF cytokine therapy. *Lancet.* 2004;363:746–747.
25. Hill JM, Syed MA, Arai AE, Powell TM, Paul JD, Zalos G, Read EJ, Khuu HM, Leitman SF, Horne M, Csako G, Dunbar CE, Waclawiw MA, Cannon RO III. Outcomes and risks of granulocyte colony-stimulating factor in patients with coronary artery disease. *J Am Coll Cardiol.* 2005;46: 1643–8.
26. Kawachi Y, Watanabe A, Uchida T, Yoshizawa K, Kurooka N, Setsu K. Acute arterial thrombosis due to platelet aggregation in a patient receiving granulocyte colony-stimulating factor. *Br J Haematol.* 1996;94:413–416.
27. Fukumoto Y, Miyamoto T, Okamura T, Gondo H, Iwasaki H, Horiuchi T, Yoshizawa S, Inaba S, Harada M, Niho Y. Angina pectoris occuring during granulocyte colony-stimulating factor-combined preparatory regimen for autologous peripheral blood stem cell transplantation in a patient with acute myelogenous leukemia. *Br J Haematol.* 1997;97: 666–668.
28. Hierholzer C, Kelly E, Lyons V, Roedling E, Davies P, Billiar TR, Tweardy DJ. G-CSF instillation into rat lungs mediates neutrophil recruitment, pulmonary edema, and hypoxia. *J Leukoc Biol.* 1998;63: 169–174.
29. Azoulay E, Attalah H, Yang K, Jouault H, Schlemmer B, Brun-Buisson C, Brochard L, Harf A, Delclaux C. Exacerbation by granulocyte colony-stimulating factor of prior acute lung injury: implication of neutrophils. *Crit Care Med.* 2002;30:2115–2122.
30. Hardy MM, Flickinger AG, Riley DP, Weiss RH, Ryan US. Superoxide dismutase mimetics inhibit neutrophil-mediated human aortic endothelial cell injury in vitro. *J Biol Chem.* 1994;269:18535–18540.
31. Iba O, Matsubara H, Nozawa Y, Fujiyama S, Amano K, Mori Y, Kojima H, Iwasaka T. Angiogenesis by implantation of peripheral blood mononuclear cells and platelets into ischemic limbs. *Circulation.* 2002;8;106: 2019–2025.
32. Fuste B, Mazzara R, Escolar G, Merino A, Ordinas A, Diaz-Ricart M. Granulocyte colony-stimulating factor increases expression of adhesion receptors on endothelial cells through activation of p38 MAPK. *Haematologica.* 2004;89:578–585.
33. Canales MA, Arrieta R, Gomez-Rioja R, Diez J, Jimenez-Yuste V, Hernandez-Navarro F. Induction of a hypercoagulability state and endothelial cell activation by granulocyte colony-stimulating factor in peripheral blood stem cell donors. *J Hematother Stem Cell Res.* 2002;11: 675–681.
34. Kudo FA, Nishibe T, Nishibe M, Yasuda K. Autologous transplantation of peripheral blood endothelial progenitor cells (CD34+) for therapeutic angiogenesis in patients with critical limb ischemia. *Int Angiol.* 2003;22: 344–348.
35. Madeddu P, Emanueli C, Pelosi E, Salis MB, Cerio AM, Bonanno G, Patti M, Stassi G, Condorelli G, Peschle C. Transplantation of low dose CD34+KDR+ cells promotes vascular and muscular regeneration in ischemic limbs. *FASEB J.* 2004;18:1737–1739.
36. Urbich C, Dimmeler S. Endothelial progenitor cells: characterization and role in vascular biology. *Circ Res.* 2004;95:343–353.
37. Shintani S, Murohara T, Ikeda H, Ueno T, Sasaki K, Duan J, Imaizumi T. Augmentation of postnatal neovascularization with autologous bone marrow transplantation. *Circulation.* 2001;103:897–903.
38. Strauer BE, Brehm M, Zeus T, Kostering M, Hernandez A, Sorg RV, Kogler G, Wernet P. Repair of infarcted myocardium by autologous intracoronary mononuclear bone marrow cell transplantation in humans. *Circulation.* 2002;106:1913–1918.
39. Assmus B, Schachinger V, Teupe C, Britten M, Lehmann R, Dobert N, Grunwald F, Aicher A, Urbich C, Martin H, Hoelzer D, Dimmeler S, Zeiher AM Transplantation of Progenitor Cells and Regeneration Enhancement in Acute Myocardial Infarction (TOPCARE-AMI). *Circulation.* 2002;106:3009–3017.
40. Valgimigli M, Rigolin GM, Cittanti C, Malagutti P, Curello S, Castoldi G, Ferrari R. Use of granulocyte-colony stimulating factor during acute myocardial infarction to enhance bone marrow stem cell mobilization in humans: clinical and angiographic safety profile. *Eur Heart J.* 2005;26: 1838–1845.

Arteriosclerosis, Thrombosis, and Vascular Biology

JOURNAL OF THE AMERICAN HEART ASSOCIATION

Targeted Delivery of Bone Marrow Mononuclear Cells by Ultrasound Destruction of Microbubbles Induces Both Angiogenesis and Arteriogenesis Response

Takanobu Imada, Tetsuya Tatsumi, Yasukiyo Mori, Takashi Nishiue, Masayuki Yoshida, Hiroya Masaki, Mitsuhiko Okigaki, Hiroyuki Kojima, Yoshihisa Nozawa, Yasunobu Nishiwaki, Noriko Nitta, Toshiji Iwasaka and Hiroaki Matsubara

Arterioscler. Thromb. Vasc. Biol. 2005;25;2128-2134; originally published online Jul 28, 2005;

DOI: 10.1161/01.ATV.0000179768.06206.cb

Arteriosclerosis, Thrombosis, and Vascular Biology is published by the American Heart Association. 7272 Greenville Avenue, Dallas, TX 72514

 Print ISSN: 1079-5642. Online ISSN: 1524-4636

Targeted Delivery of Bone Marrow Mononuclear Cells by Ultrasound Destruction of Microbubbles Induces Both Angiogenesis and Arteriogenesis Response

Takanobu Imada, Tetsuya Tatsumi, Yasukiyo Mori, Takashi Nishiue, Masayuki Yoshida, Hiroya Masaki, Mitsuhiko Okigaki, Hiroyuki Kojima, Yoshihisa Nozawa, Yasunobu Nishiwaki, Noriko Nitta, Toshiji Iwasaka, Hiroaki Matsubara

Objective—Ultrasound (US)-mediated destruction of contrast microbubbles causes capillary rupturing that stimulates arteriogenesis, whereas intramuscular implantation (im) of bone marrow mononuclear cells (BM-MNCs) induces angiogenesis. We therefore studied whether US-targeted microbubble destruction combined with transplantation of BM-MNCs can enhance blood flow restoration by stimulating both angiogenesis and arteriogenesis.

Methods and Results—US-mediated destruction of phospholipid-coated microbubbles was applied onto ischemic hindlimb muscle and subsequently BM-MNCs were transfused. A significant enhancement in blood flow recovery after Bubble+US+BM-MNC infusion (34% increase, $P<0.05$) was observed compared with Bubble+US (25%). The ratio of capillary/muscle fiber increased by Bubble+US+BM-MNC-i.v (260%, $P<0.01$) than that in the Bubble+US group (172%), into which BM-MNCs were incorporated (angiogenesis). Smooth muscle α-actin–positive arterioles were also increased, and angiography showed augmented collateral vessel formation (arteriogenesis). Platelet-derived proinflammatory factors activated by Bubble+US induces the expression of adhesion molecules (P-selectin and ICAM-1), leading to the attachment of transplanted BM-MNCs on the endothelium. Flow assay confirmed that the platelet-derived factors cause the adhesion of BM-MNCs onto endothelium under laminar flow.

Conclusions—This study demonstrates that the targeted delivery of BM-MNCs by US destruction of microbubbles enhances regional angiogenesis and arteriogenesis response, in which the release of platelet-derived proinflammatory factors activated by Bubble+US play a key role in the attachment of transplanted BM-MNCs onto the endothelial layer. (***Arterioscler Thromb Vasc Biol.* 2005;25:2128-2134.)**

Key Words: angiogenesis ■ vasculogenesis ■ stem cell ■ endothelial progenitor cell ■ ultrasound

Therapeutic angiogenesis, the ability to induce the formation of new blood vessels, is one of the most promising targets for regeneration therapy. To induce angiogenesis, investigators have delivered vascular endothelial growth factor (VEGF), basic fibroblast growth factor (bFGF/FGF2). or hypoxia-inducible factor-1α/etoposide as recombinant proteins or genes.[1] Intramuscular injection of bone marrow mononuclear cells (BM-MNCs) was shown to be feasible in patients or animals with ischemic limbs by supplying angiogenic factors and endothelial progenitors.[2–4] A noninvasive cell delivery system that can target vascular endothelium would be a great advantage for manipulation of angiogenic cell therapy.

Ultrasound (US)-targeted microbubble destruction has been investigated as a new method for delivering drugs and genes to specific tissues.[5–11] This method involves the attachment of drugs or genes to gas-filled microbubbles, which are then circulated through the intravascular space and mechanically destroyed within the target organ. Theoretically, one can target any anatomic site that is accessible by US, including selected damaged regions.[5–11] Song et al have reported that US-targeted microbubble destruction causes capillary rupturing that stimulates arteriogenesis and an increase in blood flow in both normal[12] and ischemic[13] skeletal muscles, in which angiogenesis response is transient and unlikely contributes to chronic restoration of blood flow. We previously demonstrated that the recruitment of BM-MNCs and platelets stimulates angiogenesis response in ischemic muscles by releasing potent angiogenic factors, such as VEGF or bFGF, and supply of endothelial progenitors.[3,14] Furthermore, we have recently reported that systemically

Original received December 27, 2004; final version accepted May 18, 2005.

From the Department of Medicine II (T. Imada, Y.M., T.N., H. Masaki, T. Iwasaka) and Radiology (H.K.), Kansai Medical University, Osaka; the Department of Cardiovascular Medicine (T.T., M.O., H. Matsubara), Kyoto Prefectural University School of Medicine, Kyoto; the Department of Medical Biochemistry (M.Y., Y. Nishiwaki, N.N.), Graduate School of Medicine, Tokyo Medical and Dental University, Tokyo; and the Pharmacobioregulation Research Laboratory (Y. Nozawa), Taiho Pharmaceutical Co Ltd, Saitama, Japan.

T. Iwasaka and H. Matsubara contributed equally to this study.

Correspondence to Hiroaki Matsubara MD, Department of Cardiovascular Medicine, Kyoto Prefectural University School of Medicine, Kamigyo-ku, Kyoto, 602-8566, Japan. E-mail matsubah@koto.kpu-m.ac.jp

Arterioscler Thromb Vasc Biol. **is available at http://www.atvbaha.org** **DOI: 10.1161/01.ATV.0000179768.06206.cb**

transplanted BM-MNCs can be firmly attached onto the injured vascular endothelium in an adhesive molecule–dependent manner.[15] We therefore examined whether US-targeted microbubble destruction combined with intravenous transplantation of BM-MNCs causes angiogenesis response as well as arteriogenesis in a rat model with an ischemic hindlimb, leading to an enhancement of chronic blood flow restoration. Interestingly, we found that platelet-derived factors activated by US-targeted microbubble destruction induce the expression of adhesive molecules on the endothelium and subsequent attachment of transplanted BM-MNCs, resulting in an enhancement of formation of neocapillaries and new arterioles and an increase in regional blood flow recovery.

Materials and Methods

Microbubble Preparations

BR14 (Bracco Diagnostics) is a new ultrasound contrast agent, consisting of perfluorocarbon-containing microbubbles stabilized by a phospholipid monolayer.[16,17] The suspension of gas microbubbles is reconstituted immediately before use by injecting 5 mL of 0.9% sodium chloride. The mean diameter of bubbles is 2.3 to 2.5 μm and the bubble concentration is $\approx 6\times10^8$ per ml. BR14 was administered as a 1 mL bolus injection via contralateral femoral vein.

Isolation of BM-MNC and Characterization of Endothelial-Lineage Cells

BM-MNCs were isolated from SEA/LEW rat femoral bone and centrifuged by density gradient (Lymphoprep; Nycomed). The MNC fraction was labeled with red-fluorescence cell linker (PKH26-GL; Sigma).[2,3,14] Endothelial lineage cells were analyzed by fluorescence-activated cell sorter (FACS) using DiI-acetylated LDL (acLDL) incorporation (Biogenesis) and Ulex lectin binding (Sigma) as described previously.[2,3,14]

Hindlimb Ischemia, US Application, and Transfusion of BM-MNCs

Unilateral hindlimb ischemia was induced by resecting the left femoral artery as described.[2,18] Arteriogenesis that restores the regional blood flow was reported to be observed 3 days after induction of limb ischemia of rats.[12,13] We therefore performed the infusion of microbubble at day 3 after limb ischemia to efficiently deliver microbubble BR14 to the ischemic site. We divided the rats into the following five groups: (1) Control (saline injection, n=8); (2) Bubble (1 mL BR14)+US (n=8); (3) Bubble+US+BM-MNC-i.v. (n=8), BM-MNC (2×10^7 in 1 mL saline) injected from contralateral femoral vein 1 minute after Bubble+US; (4) BM-MNC-i.m. (n=8), BM-MNC (2×10^7) intramuscularly implanted into the ischemic limb; and (5) BM-MNC-i.v. (n=8); BM-MNC (2×10^7 in 1 mL saline). BM-MNC (2×10^7) included $0.3\pm0.04\times10^7$ platelets.

The skin overlying the ischemic thigh muscle to be treated was reflected back, ultrasound gel was placed over the ischemic muscle, and 1-MHz transducer (S-probe, Effective Radiating Area: 0.9 cm^2; Ito Co Ltd) was held 3 mm over the muscle and to keep the skin temperature around $\approx$37°C. A continuous sinusoidal wave ultrasound (1MHz, 2W/cm^2, Beam Nonuniformity Ratio: 3.6; ITO-US-700) was applied for 1 minute immediately after microbubble injection. To clarify whether the microbubbles really reach ischemic tissues after infusion from contralateral femoral vein, the delivery of injected microbubbles to the ischemic area was examined by a diagnostic ultrasound echography (Sonos-5500) equipped with an ultraband S12 sector transducer.

Evaluation of Neocapillary and Immunohistochemical Analysis

Four pieces of ischemic tissues from the adductor and semimembranous muscles were obtained 28 days after limb ischemia. Frozen sections were stained with antibodies for smooth muscle (SM) α-actin (Sigma) and anti-factor VIII (DAKO) antibodies. The appropriate secondary antibodies conjugated with fluorescein isothiocyanate (FITC) or rhodamine were used. Ten fields from 2 muscle samples of each animal were randomly selected for the vessel count. To ensure that vessel densities were not overestimated as a consequence of myocyte atrophy or underestimated because of interstitial edema, the capillary/muscle fiber ratio was determined.[3,18]

Electron Microscope

Femoral arteries in skeletal muscles on which targeted US was applied were isolated after Bubble+US treatment (n=4), fixed by 2.5% glutaraldehyde and 1.5% osmium acid, dried, and viewed by electron microscope (HITATI S-700).[15]

Cell Culture and Platelet-Rich Plasma Isolation

Human umbilical vein endothelial cells (HUVECs; Kurabo) were cultured in HuMedia-EG2 medium. For use in the study apparatus, HUVECs (2nd or 3rd passages) were plated on 22-mm fibronectin-coated cover slips.[15] Peripheral blood was drawn from healthy volunteers and mixed with 0.1 volume of citrate (108 mmol/L). Whole blood was centrifuged at 150g for 10 minutes to harvest platelet-rich plasma (PRP).

Adhesion Assay Under Laminar Flow and Immunofluorescence Study

HUVECs were incubated for 30 minutes with serum-free medium with or without freshly prepared 10% platelet-rich plasma, and then stimulated by (1) 10% Bubble+US (1MHz, 1.5W, 30 seconds) in 10% PRP (Bubble+US with platelet group), (2) 10% Bubble+US in PRP (Bubble+US without platelet), (3) incubation media (in which 10% platelet-rich medium was stimulated by 10% Bubble+US), or (4) US with platelet (in which 10% platelet-rich medium was stimulated by US alone), n=6 in each experiment. HUVECs were placed on the cold plate to prevent the heating by the US, and adhesion assay under laminar flow was performed as previously described.[15] For further detail, please see the supplemental Methods, available online at http://atvb.ahajournals.org.

Stimulated HUVECs were fixed by 4% paraformaldehyde 1 hour after stimulation and incubated with anti–P-selectin (R&D Systems, Inc) and anti-platelet glycoprotein (GP)-Ib antibody (DAKO). The appropriate secondary antibodies conjugated with FITC or rhodamine were used. Nuclei were stained with 4′,6′-diamidino-2-phenylindole dihydrochloride (DAPI) and viewed by a fluorescence microscope (Olympus OX71).

Laser Doppler Perfusion Image and Angiography

Laser doppler perfusion image (LDPI) and angiography were performed as previously described[3,18] For further detail, please see the supplemental Methods.

Statistical Analysis

Statistical analyses were performed with 1-way ANOVA followed by pair-wise contrasts using the Dunnett test. Data (mean±SE) were considered statistically significant when $P<0.05$.

Results

Incidence of Endothelial-Lineage Cells in BM-MNCs

FACS analysis indicated that 28±1.8% and 31±1.5% of BM-MNCs incorporated DiI-acLDL and bound Ulex-lectin (n=5), respectively, and 20±1.2% of cells were positive for both markers. Endothelial-lineage cells were considered to be included in this fraction as reported.[2,3,14]

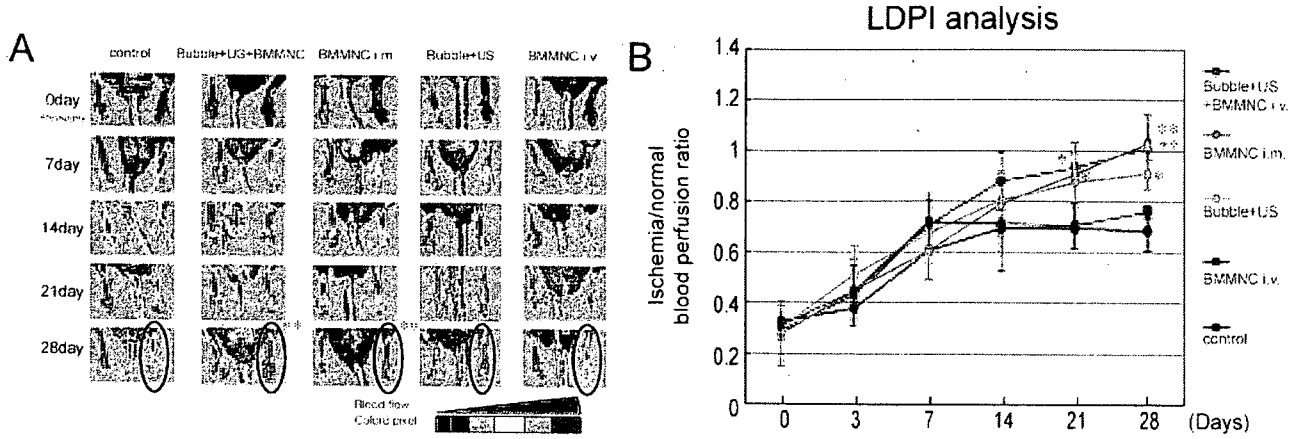

Figure 1. Increase of blood flow by US-microbubble-mediated transfusion of BM-MNCs. A, Representative LDPI. Greater blood perfusion (red to yellow) in ischemic limbs was observed in Bubble+US+BM-MNC infusion, BM-MNC-i.m., and Bubble+US groups in contrast with the untreated control and BM-MNC-i.v. groups. B, Computer-assisted analyses of LDPI revealed a significantly greater blood perfusion in the Bubble+US+BM-MNC-i.v., BM-MNC-i.m., and Bubble+US groups than in the control group. The values shown are mean±SE (n=8) at each time point. *$P<0.05$, **$P<0.01$ vs control.

Laser Doppler Blood Perfusion

Subcutaneous blood perfusion was analyzed by LDPI imaging (Figure 1). Intravenous injection of BM-MNCs (BM-MNC-i.v.) did not cause a significant increase in the blood flow recover compared with the control (saline injection; Figure 1). Treatment with Bubble+US without BM-MNCs-i.v. showed a moderate increase (25±2% at Day 28 versus control, $P<0.05$), whereas the combination of Bubble+US and BM-MNCs-i.v. induced a further increase (34±2% versus control at Day 28, $P<0.01$), which was significantly higher than that of Bubble+US manipulation alone ($P<0.05$). The blood perfusion recovery by Bubble+US+BM-MNC-i.v. was comparable to blood perfusion by BM-MNC-i.m. (38±3%). Blood perfusion after US+BM-MNC-i.v. without Bubble did not significantly differ from those in BM-MNC-i.v. alone or control groups (3±1% versus control at Day 28, n=8; data not shown), suggesting that the combination of BM-MNCs infusion with Bubble+US significantly improves the blood flow recovery after limb ischemia compared with each manipulation alone, and that the efficient cell delivery system depends on US-mediated destruction of microbubbles.

Neocapillary and Arteriole Formation

Formation of capillaries and arterioles was evaluated by factor VIII–positive and SM α-actin–positive vessels. The ratio of capillary/muscle fiber (factor VIII–positive and SM α-actin–negative vessel) was significantly increased in the Bubble+US+BM-MNC-i.v. group (260±15% versus control, $P<0.01$), which was greater ($P<0.01$) than that of Bubble+US group (172±11% versus control, $P<0.05$). The ratio of arteriole/muscle fiber (factor VIII–positive and SM α-actin–positive vessel) was also increased by Bubble+US+BM-MNC-i.v. (188±10% versus control, $P<0.01$), which was greater ($P<0.05$) than that in the Bubble+US group (146±9% versus control, $P<0.05$; Figure 2A). Transfused BM-MNCs (labeled with red fluorescence) were found to be incorporated into microvessels by Bubble+US+BM-MNC-i.v. (arrows in Figure 2B). These findings suggest that Bubble+US+BM-MNC-i.v. enhances both angiogenesis as well as arteriogenesis response.

To examine the specificity of this cell delivery system, we examined the distribution of transfused BM-MNCs in other tissues (kidney, spleen, liver, heart, pancreas, small intestines, and brain) 3 weeks after targeted cell delivery by Bubble+US+BM-MNCs-iv. Small numbers of labeled BM-MNCs were detected in the kidney (mainly in the tubule) and greater numbers of BM-MNCs were observed in the spleen, whereas no labeled cells were detected in other tissues (Figure I, available online at http://atvb.ahajournals.org).

Arteriogenesis Response Evaluated by Angiography

Compared with angiogenesis formed by capillary sprouting, arteriogenesis is often studied with the use of angiography. On the postoperative day 28, all animals were subjected to iliac angiography. Representative angiograms (n=4 in each group) are shown in Figure II (available online at http://atvb.ahajournals.org), in which arrows indicate the ligated ends of femoral arteries. Collateral vessels in the thigh area were quantitatively counted using 5-mm^2 grids.[3,18] An apparent increase in collateral vessel formation was observed in the Bubble+US+BM-MNC-i.v. and BM-MNC-i.m. (4.2±0.2-fold and 4.3±0.2-fold, n=6, respectively; $P<0.001$) compared with that in the BM-MNC-i.v. group. The increase in the Bubble+US group was 1.8±0.1-fold ($P<0.05$) when compared with that in the BM-MNC-i.v. group, which was significantly smaller ($P<0.01$) than that of the Bubble+US+BM-MNC-i.v. group. There was no significant difference between control (saline infusion) and BM-MNC-i.v. groups.

Delivery of Microbubbles to the Ischemic Muscle

Arteriogenesis that restores the regional blood flow was observed 3 days after induction of limb ischemia of rats.[12,13] We therefore performed the infusion of microbubble at day 3 after limb ischemia to efficiently deliver microbubble BR14

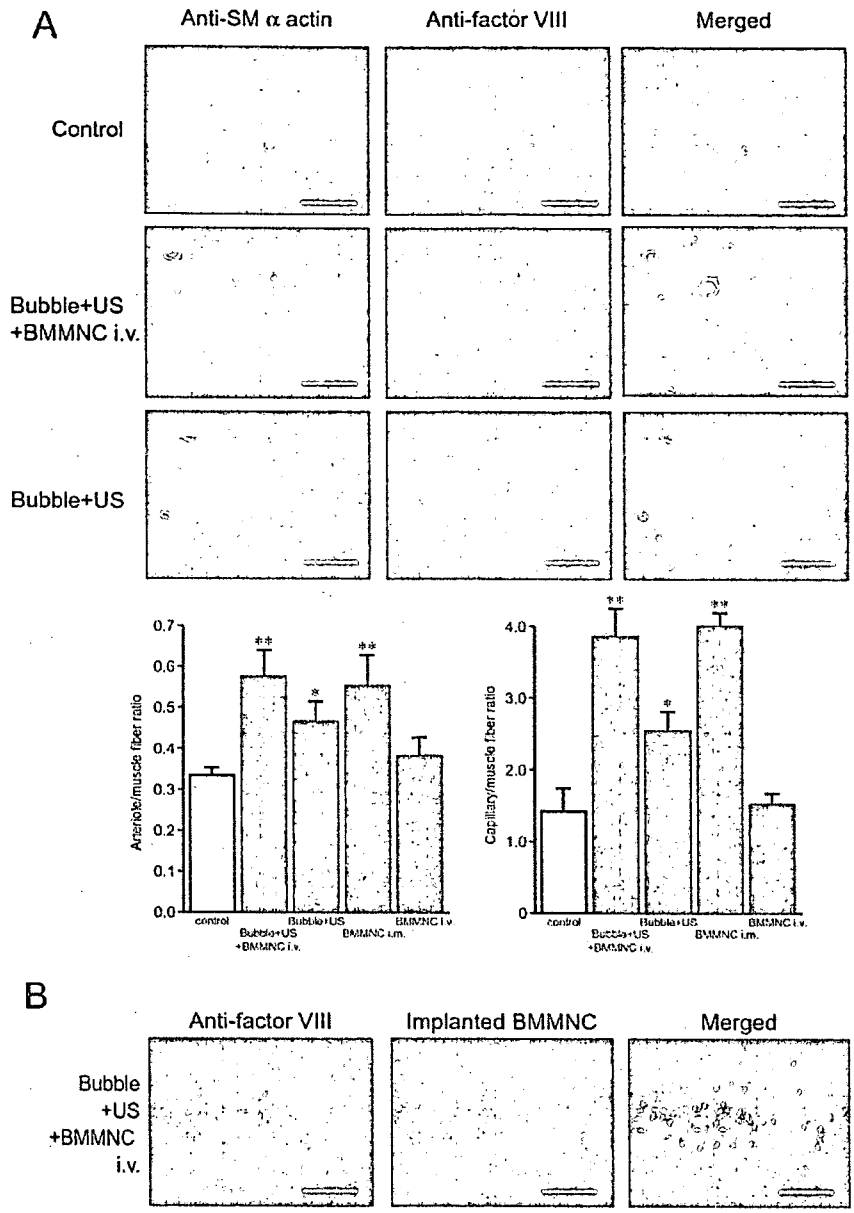

Figure 2. Formation of arterioles/capillaries and incorporation of transfused BM-MNCs. A, Vessels were immunostained with anti-SM α-actin and anti-factor VIII antibodies. Numbers for arterioles (positive for both SM α-actin and factor VIII staining) and capillaries (SM α-actin–negative and factor VIII–positive) were evaluated as a vessel number/muscle fiber ratio (n=8, each group). $^{*}P<0.05$, $^{**}P<0.01$ vs the saline-injected control. Bar=50 μm. B, Incorporation of transfused BM-MNCs (labeled with red-fluorescence). Red-labeled cells were incorporated into factor VIII–positive capillaries (arrows in the merged image) in the Bubble+US+BM-MNC-i.v. group. Data shown are representative of 5 different animals. Bar=200 μm.

to the ischemic site. We further examined whether the transfused microbubbles really reach the hindlimb muscle at 3 days after induction of ischemia. Apparent increase in the contrast densities in the ischemic thigh muscle (indicated by arrows in Figure III, available online at http://atvb.ahajournals.org) was observed ≈15 seconds after injection of microbubbles in both control (normal) and ischemic limbs compared with the pre-images before injection of microbubbles. The increase in contrast shadow diminished after 1 minute of US stimulation, indicating that microbubbles really reach ischemic hindlimb muscles after venous infusion.

Electromicroscopy

A previous study reported the presence of small holes in the endothelial cells treated with Bubble+US,[11] whereas we could not detect the presence of apparent small holes in the vascular endothelium in the skeletal muscle on which the Bubble+US was applied. Neither adhesion of MNCs nor formation of fibrin network including platelets was detected on the surface of normal endothelium or endothelium stimulated by US without microbubbles. Interestingly, we found the attachment of platelets associated with fibrin network and MNCs on the surface of endothelium in all arteries treated by Bubble+US+BM-MNCs infusion (n=6; Figure 3), whereas no adhesion of platelets or MNCs was detected in the US+BM-MNC group without microbubbles (n=6; data not shown).

Induction of Adhesion Molecules

We have reported that transplanted BM-MNCs can firmly attach onto the injured vascular endothelium in an adhesive molecule–dependent manner.[15] We therefore examined the expression profile of adhesive molecules on HUVECs treated by Bubble+US. The expression of adhesive molecules (P-selectin or ICAM-1) was not induced when HUVECs were

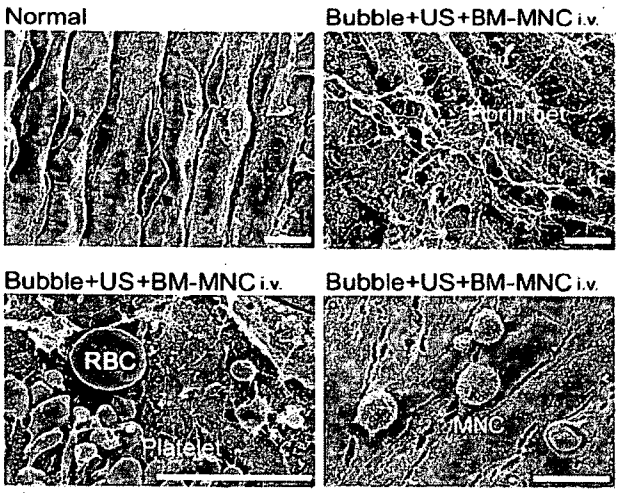

Figure 3. Electron-microscopic appearance of endothelium stimulated by Bubble-US+BM-MNCs. Electron-microscopy showing normal endothelium covered with a monolayer coat (Normal) and appearance of Bubble+US+BM-MNCs i.v.-stimulated endothelium. Attachment of both platelets associated with fibrin network and MNCs was observed on all samples treated by Bubble+US+BM-MNCs i.v. Representative figures are shown (n=4 in each group). Bar=10 μm.

stimulated by Bubble+US in the medium without platelets. Because we found that adhesion of the fibrin network including platelets was consistently observed on the surface of endothelium in all Bubble+US-treated samples (Figure 3), we next examined the involvement of platelet-derived factors in the adhesion of BM-MNCs. Interestingly, the expression of P-selectin (red fluorescence, right panel in Figure 4) and ICAM-1 was markedly induced in both HUVECs and attaching glycoprotein Ib–positive platelets (merged, yellow), when HUVECs were stimulated by Bubble+US in the medium including platelets (only P-selectin data shown in Figure 4).

We also studied whether factors released from the platelets stimulated by Bubble+US are involved in the induction of adhesion molecules. Therefore, we examined the effect of the incubation medium, in which platelet-including medium was stimulated by Bubble+US, on the induction of adhesion molecules. The addition of incubation medium caused the apparent increase in P-selectin expression on HUVECs (red fluorescence, right panel in Figure 4), suggesting that the factors released from the platelets stimulated by Bubble+US are closely involved in the induction of adhesion molecules on HUVECs. Treatment of HUVECs by US alone without microbubbles in the medium including platelets did not induce any expression of adhesive molecules (data not shown). These findings suggest that activation of platelets by Bubble+US and release of platelet-derived proinflammatory factors play a key role in the induction of adhesion molecules in the endothelial cells.

Laminar Flow Assay

We next studied whether the adhesive activity of BM-MNCs on the endothelium was actually modulated by Bubble+US-activated platelets under laminar flow condition. HUVECs were stimulated by Bubble+US in the medium containing platelets and then the adhesion ratio of BM-MNCs on HUVECs was evaluated under laminar flow as previously reported.[15] The presence of platelets in the medium markedly increased the adhesion ratio of BM-MNCs (3.5-fold, $P<0.01$) compared with Bubble+US without platelets (Figure 5). Moderate increase (1.9-fold, $P<0.01$) was observed in the incubation medium group (in which medium including platelets was stimulated by Bubble+US and then added to HUVECs) compared with the ratio in the untreated HUVECs (control). Treatment of HUVECs by US stimulation without microbubbles in the medium including platelets or addition of control medium including platelet alone (without US stimulation) did not cause a significant increase in the adhesion ratio of BM-MNCs compared with the ratio in the untreated HUVEC (data not shown).

Discussion

Angiogenic cell therapy by intramuscular implantation of autologous BM-MNCs was shown to be feasible in patients with ischemic limbs.[2] Because intramuscular implantation is

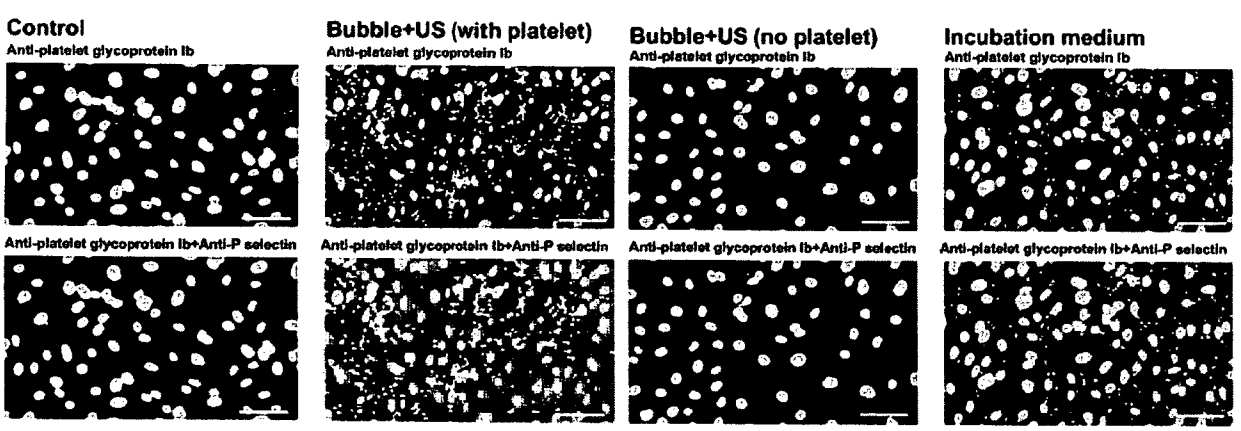

Figure 4. Adhesion of platelets and induction of adhesion molecules on Bubble+US-stimulated HUVECs. The presence of platelets and expression of P-selectin are shown by immunostaining with anti–GP-Ib (green fluorescence) and anti–P-selectin (red fluorescence) antibodies and DAPI staining (blue fluorescence). The expression of P-selectin and adhesion of platelets were observed on HUVECs, when HUVECs were stimulated by Bubble+US in the medium containing 10% platelets or exposed to the incubation medium (in which 10% platelet-including medium was stimulated by Bubble+US). The expression of P-selectin (red fluorescence) on HUVECs and attaching platelets was markedly induced. Bar=50 μm.

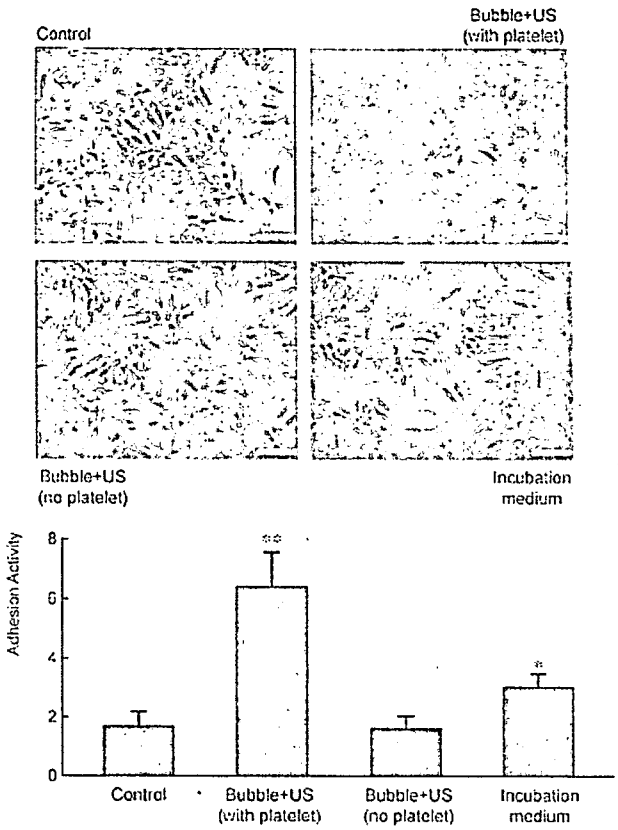

Figure 5. Laminar flow assay of BM-MNCs adhesion. Adhesive activities of BM-MNCs were quantified on HUVEC monolayer under laminar flow. Adhesive cells are indicated by yellow arrows. Cells were considered to be adherent after 10 seconds of stable contact with the monolayer. HUVECs were stimulated by Bubble+US (1MHz, 1.5W, 30 seconds) in the medium with 10% platelets (n=6), without platelets (n=6), or in the incubation medium (in which 10% platelet-including medium was stimulated by Bubble+US, n=6). $^{*}P<0.05$, $^{**}P<0.01$ vs the untreated control. Bar=100 μm.

invasive at the injected sites, the development of a noninvasive cell delivery system that can target vascular endothelium would be a great advantage for the manipulation of angiogenic cell therapy. A new delivery system of drugs or genes has been developed using US-targeted microbubble destruction; the drugs or genes that attach onto gas-filled microbubbles circulate through the intravascular space and are mechanically destroyed within the target organ by ultrasound,[5–11] whereas no studies were reported to determine whether this method is feasible for delivering the "cells" to specific vascular sites.

US-targeted microbubble destruction was reported to cause an inflammatory action on the cell surface by making small holes that revert to a normal appearance within 24 hours.[10,11] Song et al have reported that US-targeted microbubble destruction causes capillary rupturing that stimulates arteriogenesis and an increase in blood flow in both normal[12] and ischemic[13] skeletal muscles, in which angiogenesis response is transient and unlikely contributes to chronic restoration of blood flow. They concluded that arteriogenesis response rather than angiogenesis plays a major role in US+microbubble-stimulated blood flow recovery. We previously demonstrated that the recruitment of BM-MNCs and platelets stimulates angiogenesis response in the ischemic muscles by releasing potent angiogenic factors, such as VEGF or bFGF, and supply of endothelial progenitors.[3,14] Furthermore, we have recently reported that systemically transplanted BM-MNCs can be firmly attached onto the injured vascular endothelium in an adhesive molecule–dependent manner.[15] We therefore expanded the previous studies by Song et al[12,13] and examined whether US-targeted microbubble destruction combined with intravenous transplantation of BM-MNCs causes both angiogenesis and arteriogenesis response in an ischemic hindlimb model, leading to a greater enhancement of blood flow restoration.

We found that (1) intravenous infusion of BM-MNCs combined with US-mediated destruction of microbubbles markedly enhances the restoration of regional blood perfusion in ischemic hindlimbs by stimulating both chronic angiogenesis and arteriogenesis response, and (2) release of platelet-derived proinflammatory factors activated by US-mediated destruction of microbubbles causes the adhesion of transfused BM-MNCs on endothelium by inducing the expression of adhesion molecules (P-selectin and ICAM-1). We found that BM-MNCs transfused intravenously were trapped by the spleen and a few BM-MNCs were present in the renal tubules. Considering that BM-derived hematopoietic stem cells were reported to transdifferentiate to renal tubular cells and improve renal function in the ischemia-reperfusion injury model,[19] the present study establishes for the first time that targeted delivery of BM-MNCs by US destruction of microbubbles is an efficient cell delivery system for therapeutic angiogenesis and arteriogenesis, and that the presence of platelets and/or platelet-derived proinflammatory factors activated by US+microbubbles play an important role in the targeted adhesion of BM-MNCs on vascular endothelium.

Previous studies have indicated that platelet attachment to an inter- or sub-endothelial matrix of endothelial cells promotes selectin-mediated leukocyte adhesion to the damaged endothelium under the flow assay condition.[20,21] Inhibition of P-selectin caused a marked inhibition of leukocyte adhesion at a high shear stress.[20] P-selectin is a receptor for leukocytes and monocytes when its expression is induced on activated platelets and endothelium. This property facilitates rapid adhesion of leukocytes to endothelium in injury tissue regions and enhances platelet-leukocyte interactions at sites of inflammation. Endothelial P-selectin is located on membranes of Weibel-Plade bodies, the secretory granules of endothelium in which large multimers of von Willebrand factor (vWF) are stored.[22] After cellular stimulation with agonists such as thrombin or histamine, P-selectin is rapidly expressed on the endothelial cell surface, making it an excellent candidate for directing adherence of unstimulated leukocytes toward endothelium within minutes of tissue injury.[23] Furthermore, we have reported that BM-MNCs have a higher rolling and adhesive activities because of the greater expressions of adhesive molecules such as P-selectin compared with peripheral blood-derived leukocytes.[15] In this study, we found that factors released from platelets stimulated by microbubble destruction are responsible for the attachment of platelets and BM-MNCs onto the endothelium and the induction of endothelial P-selectin and ICAM-1. The present data from the flow assay also confirm that platelet-derived factors play a key role for adhesion of BM-MNCs onto the endothelial cells under

laminar flow. Although we previously showed that platelet-derived VEGF is mainly associated with the angiogenesis response by platelet implantation,[3] preincubation with antibodies for VEGF, bFGF, or PDGF-BB showed no influence on the induction of endothelial P-selectin and ICAM-1 (unpublished observation). Further studies will be required to identify the platelet-derived proinflammatory cytokines responsible for induction of endothelial adhesion molecules. Taken together, these findings suggest that release of platelet-derived proinflammatory factors and direct interaction of platelet onto the endothelial matrix, initiated by US-microbubble destruction, is an underlying mechanism for adhesion of the transfused BM-MNCs on the endothelium under shear stress.

The previous studies showed that US-mediated destruction of microbubbles induces arteriogenesis response in the skeletal muscle, whereas angiogenesis response is transient and unlikely contributes to the increase in the regional blood flow.[12] The arteriogenesis response consists of the formation of new arterioles, which presumably occurs when preexisting capillaries acquire SM coating, and an increase in the diameter of these newly formed and/or preexisting arterioles into channels with larger diameters.[13] Compared with angiogenesis formed by capillary sprouting, arteriogenesis is often studied with the use of conventional angiography. Our angiography finding is consistent with the arteriogenesis response, and the immunohistological data suggest the angiogenesis and arteriogenesis response as evaluated by the increases in capillary numbers and SM coated arterioles, respectively. The neocapillary formation was observed in the day 28 samples, suggesting that the angiogenesis is a chronic response in our study. The controversy with the studies by Song et al[12,13] may be attributable to the difference in the used microbubbles (albumin-coated Optison versus phospholipids-coated BR14). Recruitment of monocytes triggered by monocyte chemoattractant protein-1 was shown to induce arteriogenesis in inflammatory ischemic sites.[24] Because BM-MNCs contain monocyte-lineage progenitor cells,[15] it is plausible that recruitment of BM-MNCs contributes to arteriogenesis together with inflammation response by US+microbubble-mediated capillary rupturing.

In conclusion, the present study demonstrates that intravenous transfusion of BM-MNCs combined with US-destruction of microbubbles is an efficient targeted cell delivery system for therapeutic angiogenesis as well as arteriogenesis, in which the release of platelet-derived proinflammatory factors activated by Bubble+US plays a key role in the attachment of transplanted BM-MNCs onto the endothelial layer.

Acknowledgments

This study was supported in part by research grants from the Ministry of Education, Science, Sports, and Culture, Japan, the Study Group of Molecular Cardiology, the Japan Medical Association, Japan Smoking Foundation, and the Japan Heart Foundation.

References

1. Isner JM, Vale PR, Symes JF, Losordo DW. Assessment of risks associated with cardiovascular gene therapy in human subjects. *Circ Res.* 2001;89:389–400.
2. Tateishi-Yuyama E, Matsubara H, Murohara T, Ikeda U, Shintani S, Masaki H, Amano K, Kishimoto Y, Yoshimoto K, Akashi H, Shimada K, Iwasaka T. Therapeutic angiogenesis for patients with limb ischemia by autologous transplantation of bone-marrow cells: a pilot study and randomized controlled trial. *Lancet.* 2002;360:427–435.
3. Iba O, Matsubara H, Nozawa Y, Fujiyama S, Amano K, Mori Y, Kojima H, Iwasaka T. Angiogenesis by implantation of peripheral blood mononuclear cells and platelets into ischemic limbs. *Circulation.* 2002;106:2019–2025.
4. Shintani S, Murohara T, Ikeda H, Ueno T, Sasaki K, Duan J, Imaizumi T. Augmentation of postnatal neovascularization with autologous bone marrow transplantation. *Circulation.* 2001;103:897–903.
5. Bekeredjian R, Chen S, Frenkel PA, Grayburn PA, Shohet RV. Ultrasound-targeted microbubble destruction can repeatedly direct highly specific plasmid expression to the heart. *Circulation.* 2003;108:1022–1026.
6. Price RJ, Skyba DM, Kaul S, Skalak TC. Delivery of colloidal particles and red blood cells to tissue through microvessel ruptures created by targeted microbubble destruction with ultrasound. *Circulation.* 1998;98:1264–1267.
7. Lawrie A, Brisken AF, Francis SE, Tayler DI, Chamberlain J, Crossman DC, Cumberland DC, Newman CM. Ultrasound enhances reporter gene expression after transfection of vascular cells in vitro. *Circulation.* 1999;99:2617–2620.
8. Shohet RV, Chen S, Zhou YT, Wang Z, Meidell RS, Unger RH, Grayburn PA. Echocardiographic destruction of albumin microbubbles directs gene delivery to the myocardium. *Circulation.* 2000;101:2554–2556.
9. Lindner JR, Kaul S. Delivery of drugs with ultrasound. *Echocardiography.* 2001;18:329–337.
10. Teupe C, Richter S, Fissthaler B, Randriamboavonjy V, Ihling C, Fleming I, Busse R, Zeiher AM, Dimmeler S. Vascular gene transfer of phosphomimetic endothelial nitric oxide synthase (S1177D) using ultrasound-enhanced destruction of plasmid-local microbubbles improves vasoreactivity. *Circulation.* 2002;105:1104–1109.
11. Taniyama Y, Tachibana K, Hiraoka K, Namba T, Yamasaki K, Hashiya N, Aoki M, Ogihara T, Kaneda Y, Morishita R. Local delivery of plasmid DNA into rat carotid artery using ultrasound. *Circulation.* 2002;105:1233–1239.
12. Song J, Qi M, Kaul S, Price RJ. Stimulation of arteriogenesis in skeletal muscle by microbubble destruction with ultrasound. *Circulation.* 2002; 106:1550–1555.
13. Song J, Cottler PS, Klibanov AL, Kaul S, Price RJ. Microvascular remodeling and accelerated hyperemia blood flow restoration in arterially occluded skeletal muscle exposed to ultrasonic microbubble destruction. *Am J Physiol.* 2004;287:H2754–H2761.
14. Kamihata H, Matsubara H, Nishiue T, Fujiyama S, Tsutsumi Y, Ozono R, Masaki H, Mori Y, Iba O, Tateishi E, Kosaki A, Shintani S, Murohara T, Imaizumi T, Iwasaka T. Implantation of autologous bone marrow mononuclear cells into ischemic myocardium enhances collateral perfusion and regional function via side-supply of angioblasts, angiogenic ligands and cytokines. *Circulation.* 2001;104:1046–1052.
15. Fujiyama S, Amano K, Uehira K, Yoshida M, Nishiwaki Y, Nozawa Y, Jin D, Takai S, Miyazaki M, Egashira K, Imada T, Iwasaka T. Bone marrow monocyte lineage cells adhere on injured endothelium in a monocyte chemoattractant protein-1-dependent manner and accelerate reendothelialization as endothelial progenitor cells *Circ Res.* 2003;93:980–989.
16. Fisher NG, Christiansen JP, Leong-Poi H, Jayaweera AR, Linder JR, Kaul S. Myocardial and microcirculatory kinetics of BR14, a novel third-generation intravenous ultrasound contrast agent. *J Am Coll Cardiol.* 2002;39:530–537.
17. Fisher NG, Leong-Poi H, Sakuma T, Rim SJ, Bin JP, Kaul S. Detection of coronary stenosis and myocardial viability using a single intravenous bolus injection of BR14. *J Am Coll Cardiol.* 2002;39:523–529.
18. Amano K, Matsubara H, Iba O, Okigaki M, Fujiyama S, Imada T, Kojima H, Nozawa Y, Kawashima S, Yokoyama M, Iwasaka T. Enhancement of ischemia-induced angiogenesis by eNOS overexpression. *Hypertension.* 2003;41:156–162.
19. Lin F, Cordes K, Li L, Hood L, Couser WG, Shankland SJ, Igarashi P. Hematopoietic stem cells contribute to the regeneration of renal tubules after renal ischemia-reperfusion injury in mice. *J Am Soc Nephrol.* 2003;14:1188–1199.
20. Kuijper PH, Torres HG, Linden JA, Lammers JW, Sixma JJ, Koenderman L, Zwaginga JJ. Platelet-dependent primary hemostasis promotes selectin-an integrin-mediated neutrophil adhesion to damaged endothelium under flow conditions. *Blood.* 1996;87:3271–3281.
21. Theilmeier G, Lenaerts T, Remacle C, Collen D, Vermylen J, Hoylaerts MF. Circulating activated platelets assist THP-1 monocytoid/endothelial cell interaction under shear stress. *Blood.* 1999;94:2725–2734.
22. McEver RP, Beckstead JH, Moore KL, Marshall-Carlson L, Bainton DF. GMP-140, a platelet alpha-granule membrane protein, is also synthesized by vascular endothelial cells and is localized in Weibel-Palade bodies. *J Clin Invest.* 1989;84:92–99.
23. McEver RP. GMP-140: a receptor for neutrophils and monocytes on activated platelets and endothelium. *J Cell Biochem.* 1991;45:156–161.
24. Heil M, Schaper W. Influence of mechanical, cellular, and molecular factors on collateral artery growth (arteriogenesis). *Circ Res.* 2004;95:449–458.

Carbon Dioxide–Rich Water Bathing Enhances Collateral Blood Flow in Ischemic Hindlimb via Mobilization of Endothelial Progenitor Cells and Activation of NO-cGMP System

Hidekazu Irie, MD; Tetsuya Tatsumi, MD, PhD; Mitsutaka Takamiya, MD; Kan Zen, MD; Tomosaburo Takahashi, MD, PhD; Akihiro Azuma, MD, PhD; Kento Tateishi, MD; Tetsuya Nomura, MD; Hironori Hayashi, MD; Norio Nakajima, MD; Mitsuhiko Okigaki, MD, PhD; Hiroaki Matsubara, MD, PhD

Background—Carbon dioxide–rich water bathing has the effect of vasodilatation, whereas it remains undetermined whether this therapy exerts an angiogenic action associated with new vessel formation.

Methods and Results—Unilateral hindlimb ischemia was induced by resecting the femoral arteries of C57BL/J mice. Lower limbs were immersed in CO_2-enriched water (CO_2 concentration, 1000 to 1200 mg/L) or freshwater (control) at 37°C for 10 minutes once a day. Laser Doppler imaging revealed increased blood perfusion in ischemic limbs of CO_2 bathing (38% increase at day 28, $P<0.001$), whereas N^G-nitro-L-arginine methyl ester treatment abolished this effect. Angiography or immunohistochemistry revealed that collateral vessel formation and capillary densities were increased (4.1-fold and 3.7-fold, $P<0.001$, respectively). Plasma vascular endothelial growth factor (VEGF) levels were elevated at day 14 (18%, $P<0.05$). VEGF mRNA levels, phosphorylation of NO synthase, and cGMP accumulation in the CO_2-bathed hindlimb muscles were increased (2.7-fold, 2.4-fold, and 3.4-fold, respectively) but not in forelimb muscles. The number of circulating Lin−/Flk-1+/CD34− endothelial-lineage progenitor cells was markedly increased by CO_2 bathing (24-fold at day 14, $P<0.001$). The Lin−/Flk-1+/CD34− cells express other endothelial antigens (endoglin and VE-cadherin) and incorporated acetylated LDL.

Conclusions—Our present study demonstrates that CO_2 bathing of ischemic hindlimb causes the induction of local VEGF synthesis, resulting in an NO-dependent neocapillary formation associated with mobilization of endothelial progenitor cells. (***Circulation.*** **2005;111:1523-1529.**)

Key Words: carbon dioxide ◻ hypercapnia ◻ angiogenesis ◻ stem cells ◻ endothelium ◻ vasculogenesis

Carbon dioxide–rich (CO_2) water bathing has a long history and is thought to be effective in the treatment of peripheral vascular disorder[1]; however, the mechanism(s) underlying this traditional therapy remains poorly defined. The effect of CO_2-enriched water on cutaneous circulation depends primarily on the vasodilatation elicited by the CO_2 that diffuses into the subcutaneous tissue through the skin layers.[2,3] Findings in the intact coronary circulation[4] and in isolated aortic strips[5] have suggested that vasodilation in response to CO_2 may be mediated in part by nitric oxide (NO).

Previous investigations have provided inferential evidence that biological processes modulated by NO might extend to include angiogenesis. Direct in vitro evidence that NO may induce angiogenesis was demonstrated recently by Papapetropoulos et al.[6,7] Ziche et al[8,9] established the first line of evidence that NO can induce angiogenesis in vitro. Murohara et al[10] clearly showed NO-mediated angiogenesis in response to tissue ischemia in NO-deficient mice. We have also reported that overexpression of endothelial NO synthase (eNOS) causes a marked increase in neocapillary formation in response to tissue ischemia.[11] Furthermore, hypercapnia-associated acidosis was reported to induce the expression of angiogenic factors, vascular endothelial growth factor (VEGF), or basic fibroblast growth factor and inhibit endothelial cell apoptosis.[12] Taken together, this accumulated evidence may raise the possibility that the CO_2-enriched water bathing therapy enhances regional blood perfusion by increasing new vessel formation. In the present study, we report that CO_2-enriched water bathing stimulates blood flow restoration in the ischemic hindlimbs of mice by increasing NO-dependent collateral vessel formation and the mobilization of endothelial-lineage progenitor cells into the circulation.

Methods

Principle of the Device

This device uses a CO_2 gas–permeable membrane similar to the principle of an artificial lung on the extracorporeal circulatory system. The unit consists of 15 000 multilayered composite-membrane hollow fibers with porous membrane sandwiching on

Received June 1, 2004; revision received November 13, 2004; accepted November 19, 2004.

From the Department of Cardiovascular Medicine, Kyoto Prefectural University School of Medicine, Kyoto, Japan.

Correspondence to Hiroaki Matsubara, MD, Department of Cardiovascular Medicine, Kyoto Prefectural University of Medicine, Kamigyo-Ku, Kyoto, 602-8566, Japan. E-mail matsubah@koto.kpu-m.ac.jp

Circulation is available at http://www.circulationaha.org

DOI: 10.1161/01.CIR.0000159329.40098.66

both sides of gas-permeable membrane (Mitsubishi-Leiyon) and is capable of instantly converting 20 L/min of water (pH 7.0) into CO_2-enriched water (free CO_2 concentration, 1000 to 1200 mg/L, pH 5.0).

Mouse Model of Unilateral Hindlimb Ischemia and CO_2 Bathing

Unilateral hindlimb ischemia was induced by resecting the right femoral arteries (including muscle branches) and veins of 8-week-old male C57BL/J mice under anesthesia with sodium pentobarbital (50 mg/kg IP).[11,13] To inhibit NOS chronically, the mice were provided water containing 1 mg/mL N^G-nitro-L-arginine methyl ester (L-NAME) for 4 weeks.[11] Because CO_2 bathing immediately after operation delayed the closure of this skin wound, we started the CO_2 bathing of the lower limb from 4 days after surgery. Lower limbs of mice were immersed into CO_2-enriched water for 10 minutes or freshwater (control) at 37°C once a day under anesthesia (n=10 in each group). The Institutional Animal Care and Use Committee of our university approved all animal protocols.

Immunohistochemistry

Four pieces of ischemic tissues from the adductor and semimembranous muscles were obtained 28 days after the surgery of hindlimb ischemia. Frozen sections were stained with anti-factor VIII, followed by incubation with TRIC-conjugated secondary antibody. Five fields from 2 muscle samples of each animal were randomly selected for capillary counts. To ensure that capillary densities were not overestimated as a consequence of myocyte atrophy or underestimated because of interstitial edema, the capillary/muscle fiber ratio was determined.[11,13] To examine whether cells survived in the tissues, adjacent sections were subjected to alkaline phosphatase staining by the indoxyl-tetrazolium method. Alkaline phosphatase staining turns capillary endothelial cells a dark blue color only when they are viable and when the intracellular enzyme activity remains intact.[11,13]

Laser Doppler Analysis and Angiography

We measured the ratio of the ischemic (right)/normal (left) limb blood flow by use of a laser Doppler perfusion image (LDPI) analyzer (Moor Instruments). After blood flow had been scanned twice, stored images were subjected to computer-assisted quantification of blood flow, and average flows of the ischemic and nonischemic limbs were calculated. To minimize data variables caused by ambient light and temperature, the LDPI index was expressed as the ratio of ischemic (left) to nonischemic (right) limb blood flow.[11,13]

Vessel density was evaluated with a microfocus x-ray television device (Hitex Co Ltd) 28 days after ischemia (n=5). Longitudinal laparotomy was performed to introduce a catheter into the abdominal aorta, followed by injection of contrast medium (lipiodol). Angiography was performed for 2 seconds after the injection. We quantitatively analyzed collateral vessel numbers as previously reported.[11,13] Briefly, numbers of vessels in the thigh area were counted by use of 5-mm^2 grids by 2 radiologists who were unaware of the group identity of the angiographic film. Interobserver variation was <5%.

cGMP Assay and Measurement of Blood pH Level

The assay for tissue cGMP was performed by use of the cGMP enzyme immunoassay system (Biotrak; Amersham) as previously described.[11] The tissues remaining after cGMP measurement were digested by use of a bicinchoninic acid protein assay kit (Pierce). Blood pH levels were measured by automated blood gas analyzer (ABL505, Radiometer A/S).

Northern and Western Blotting and Plasma VEGF Measurement

Frozen skeletal samples from hindlimbs or forelimbs were homogenized in Trizol reagent (Gibco BRL). Blots were hybridized with a random-primed ^{32}P-labeled cDNA probe for VEGF[11] and normalized by densities for GAPDH as an internal control. Hybridized signals were measured by scanning densitometry, and VEGF mRNA levels were arbitrarily normalized relative to the GAPDH mRNA levels.

Phosphorylation of eNOS (serine 1177) was analyzed by Western blotting using phospho-specific antibodies (New England Biolabs). The muscles were homogenized in lysis buffer. Lysates were immunoblotted with anti-phospho antibodies and detected with an enhanced chemiluminescence kit (Amersham).[11] Plasma VEGF concentration was measured by use of the ELISA kit (R&D Systems).

FACS Staining

Total nuclear cells in the peripheral blood were isolated by erythrocyte lysis with ammonium chloride solution (PharM Lyse, Becton Dickinson). Lin−/Flk+ cells were isolated by PE-labeled lineage antigens (CD11b, CD3, B220, Ter-199, Gr-1, CD4, CD8e, CD16/32), FITC-CD34, and biotin-Flk-1 and then analyzed by use of a FACScan flow cytometer.[14,15] Lin−/Flk+/endoglin+ cells were isolated by FITC-labeled lineage antigens, PE–Flk-1 and biotin-endoglin. To prove the specificity of anti-CD34 antibody, the biotin-labeled anti-mouse CD34 antibody used in this study was reacted with mouse bone marrow cells and purified with streptavidin-magnet beads, followed by fluorescence-activated cell sorter (FACS) analysis using streptavidin-PE. All anti-mouse antibodies were purchased from BD Biosciences.

Differentiation of Lin−/Flk-1+ Cells Into Endothelial Cells In Vitro

The population of Lin−/Flk-1+ cells was isolated with FACS from the peripheral blood of the mice that had undergone the limb ischemic operation and then treated with CO_2 bathing for 14 days. These cells were cultured on fibronectin-coated plastic dishes in DMEM supplemented with 100 ng/mL VEGF and 10% FBS. After 4 days, DiI-labeled acetylated LDL (Biomedical Technologies Inc) was added into medium at 2 μg/mL for 6 hours, fixed with 4% paraformaldehyde, and stained with anti–VE-cadherin antibody and FITC-labeled anti-IgG antibody.

Statistics

Statistical analyses were performed by 1-way ANOVA followed by pairwise contrasts using Dunnett's test. Data (mean±SEM) were considered significant at a value of $P<0.05$.

Results

Laser Doppler Blood Perfusion

Progressive recovery of limb perfusion was disclosed in CO_2-bathed and control freshwater-bathed mice after induction of limb ischemia. A greater degree of blood perfusion recovery was observed in the ischemic limbs of CO_2-bathed mice compared with controls (38% increase at day 28, $P<0.001$) (Figure 1, A and B). Inhibition of NOS activity by L-NAME administration abolished an enhancement of blood flow recovery by CO_2 bathing and reversed the recovery ratio toward the control level. Blood flow in L-NAME–treated mice tended to be lower than that in wild-type mice, but this difference was not significant (Figure 1B).

Angiography

All animals were subjected to iliac angiography using contrast medium (lipiodol) on postoperative day 28. Collateral vessel numbers were markedly increased in ischemic limbs of CO_2-bathed mice (4.1±0.4-fold at day 28, $P<0.001$, n=5) compared with those in water-bathed mice (Figure 2).

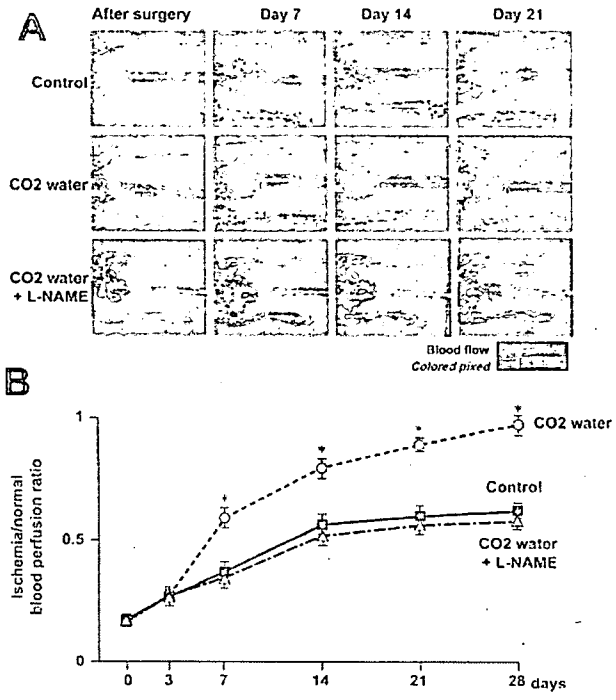

Figure 1. LDPI. A, Greater blood perfusion (red to yellow) was observed in CO_2-enriched water-bathed limbs, in contrast to reduced perfusion (green to blue) in freshwater-bathed ischemic limbs (control). B, Computer-assisted analyses of LDPI revealed significantly greater blood perfusion values in CO_2-enriched water-bathed group than in control group. Administration of L-NAME (1 mg/mL) in drinking water reduced increased perfusion by CO_2-enriched water bathing toward normal level. Values shown are mean±SEM (n=10) at each time point. *P<0.001 vs control mice.

Analysis of Capillary Density

Immunohistochemical staining for anti-factor VIII revealed the presence of capillary endothelial cells (Figure 3A). The capillary/muscle fiber ratio in the skeletal muscle obtained 28 days after hindlimb ischemia was significantly increased in the CO_2-bathed mice (3.7-fold, P<0.001) compared with that in water-bathed mice. A similar increase (4.2-fold increase, P<0.001) was also observed in ALP staining for detection of viable endothelial cells (Figure 3B). Administration of L-NAME (1 mg/mL) in drinking water reduced the increased vessel numbers by CO_2 bathing toward the normal level (Figure 3).

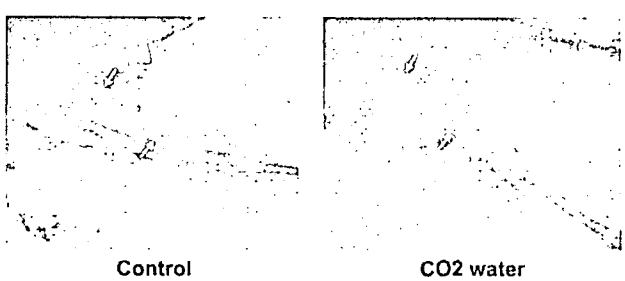

Figure 2. Angiographic analysis. Representative angiograms were obtained on postoperative day 28. Arrows indicate ligated ends of femoral arteries. Collateral vessel numbers counted by use of 5-mm² grids were markedly increased in ischemic limbs of CO_2-bathed mice (4.1±0.4-fold at day 28, P<0.001, n=5) compared with those in water-bathed mice.

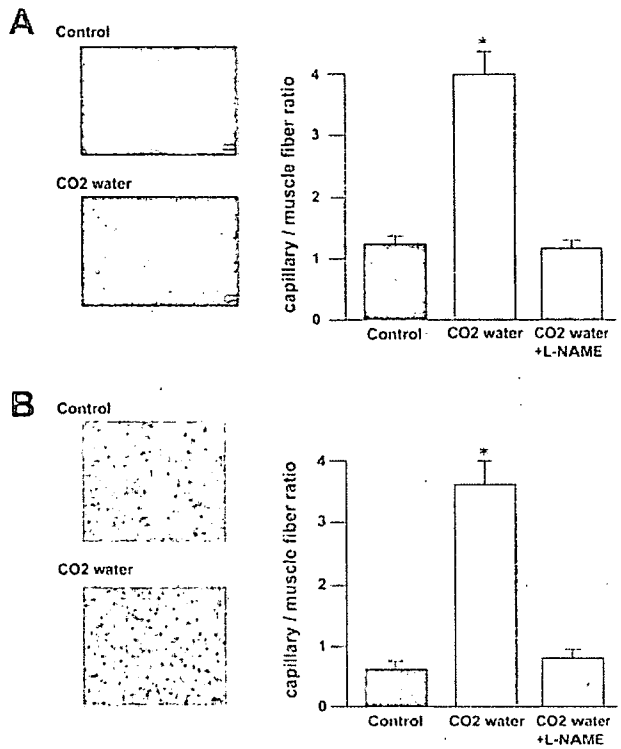

Figure 3. Immunohistochemical analysis. A, Ischemic tissues from adductor and semimembranous muscles were obtained 28 days after surgery of hindlimb ischemia. Endothelial cells were stained with anti-factor VIII antibody, followed by incubation with TRIC-conjugated secondary antisera. B, Alkaline phosphatase staining turns viable endothelial cells blue. Five fields from 2 muscle samples of each animal (n=10) were randomly selected, and capillary density was shown as capillary/muscle fiber ratio. Administration of L-NAME (1 mg/mL) in drinking water reduced increased vessel numbers by CO_2 bathing toward control levels of freshwater-bathed ischemic limbs (n=10). *P<0.001 vs control mice. Bars=50 μm.

Induction of VEGF Expression, eNOS Phosphorylation, and cGMP Levels

VEGF mRNA levels were examined in hindlimb muscles dissected at days 0 (before), 1, 2, 7, 14, and 21. VEGF mRNA levels were decreased immediately after hindlimb ischemia (day 1, day 2), and then gradually reverted to the basal levels at day 7 in the control group. In the CO_2-enriched water group, a marked increase in VEGF mRNA levels was observed at day 7 (1.6-fold versus day 0 preischemic levels, P<0.01) and showed a peak level at ≈day 14 (2.7-fold versus day 0, P<0.001). Induction of the VEGF mRNA from the preischemic level was significantly higher in the CO_2 bathing group than the increase in the control group (Figure 4), whereas the increase in VEGF mRNA synthesis by CO_2 bathing was not affected by L-NAME treatment (Figure 5A).

To define whether the effect of CO_2 bathing results from systemic or local VEGF synthesis, we examined the time-dependent VEGF mRNA induction in forelimb skeletal muscles after CO_2 bathing and changes in plasma VEGF levels. The mRNA levels in forelimb skeletal muscles of CO_2-bathed